EFFECT OF MICROWAVE IRRADIATION ON ASPECT RATIO OF TREATED MICA

by

Daniel M. Chevalier

Submitted

in partial fulfilment of the requirement

for the degree of

Master of Applied Science

Major Subject: Materials Engineering

at

DALHOUSIE UNIVERSITY

Halifax, Nova Scotia December, 2008

© Copyright by Daniel M. Chevalier 2008

Dalhousie University

Faculty of Engineering

Materials Engineering

The undersigned hereby certify that they have examined, and recommend to the Faculty of Graduate Studies for acceptance, the thesis entitled “Effect of Microwave Irradiation on Aspect Ratio of Treated Mica” by Daniel M. Chevalier in partial fulfilment of the requirements for the degree of Master of Applied Science.

Dated: December 1, 2008

Supervisor: _____
Dr. Ian Flint

Co-supervisor: _____
Dr. William Caley

Examiner: _____
Dr. Amyl Ghanem

Dalhousie University
Faculty of Engineering

DATE: December 1, 2008

AUTHOR:	Daniel M. Chevalier
TITLE:	Effect of Microwave Irradiation on Aspect Ratio of Treated Mica
MAJOR SUBJECT:	Materials Engineering
DEGREE:	Master of Applied Science
CONVOCATION:	May, 2009

Permission is herewith granted to Dalhousie University to circulate and to have copied for non-commercial purposes, at its discretion, the above thesis upon the request of individuals or institutions.

_____

Signature of Author

The author reserves other publication rights, and neither the thesis nor extracts from it may be printed or otherwise reproduced without the author's written permission.

The author attests that permission has been obtained for the use of any copyrighted material appearing in this thesis (other than brief excerpts requiring only proper acknowledgement in scholarly writing), and that all such use is clearly acknowledged.

TABLE OF CONTENTS

Page

LIST OF TABLES

LIST OF FIGURES

ACKNOWLEDGMENTS

I would like to thank my supervisor, Dr. Ian Flint, for his guidance and insight. I would also like to thank Dr. W. F. Caley and Dr. A. Ghanem for their help in this study. I must thank Dr. G. W. Kipouros for his motivational talks, his frequent inquiries of my research work were excellent reminders that kept me on track. Thomas Koch, you were very helpful with the experimental setup and imagery on the SEM.

Finally, I would like to thank my family for their patience and understanding while I was writing this. Janice, I thank you for believing in me. I could not have done it without your support.

ABSTRACT

Muscovite mica is a plate-like mineral composed of potassium and aluminum silicate. The mica morphology, characterised by aspect ratio, allows this mineral to be used as structural filler in plastics, adding rigidity and dimensional stability. In this study, two chemical leaching experiments were designed to examine their effect on mica aspect ratio. After chemical treatment, the mica underwent microwave irradiation and grinding. After leaching with concentrated HCl, the aspect ratio of mica was examined with and without microwave irradiation. In a separate experiment, the aspect ratio of mica was examined after leaching with lithium nitrate, with and without microwave irradiation. The aspect ratio of the mica was calculated by dividing the average particle size (d_{50}) of the ground mica by the average mica plate thickness. Average particle size was determined using laser diffraction, while average plate thickness was determined using SEM imagery. The HCl treatment-microwave irradiation did not increase the aspect ratio of the mica plates. However, the lithium nitrate treatment-microwave irradiation resulted in mica plates with a higher aspect ratio than lithium nitrate treatment alone.

1 Introduction

1.1 Purpose

The purpose of this research is to examine the aspect ratio of chemically treated and microwave irradiated muscovite mica. This research will determine if treating the mica with hydrochloric acid and microwave energy will produce a higher aspect ratio than when treated with hydrochloric acid alone. Similarly, this experiment will determine if treating the mica with lithium nitrate and microwave energy will produce a higher aspect ratio than when treated with lithium nitrate alone.

1.2 Scope

This experiment is designed to determine if certain chemical treatment and microwave irradiation can increase aspect ratio in muscovite mica. Based on previous research by Kalinowski et al (1996) and Caseri et al (1992), the chemical treatments are limited to hydrochloric acid and lithium nitrate solutions. The microwave oven is of a fixed power and frequency. There is no attempt made to optimise the variables in the experiment, or to evaluate the process for commercial applications.

1.3 Introduction

Muscovite mica is a plate-like mineral composed of potassium and aluminium silicate. Mica is used as filler in many applications such as crack filler, cosmetics, paints, paper, rubber, and plastics. Fillers come in intensive contact with the base matrix and they may cause a physiochemical influence on the matrix (Hohenberger et al, 2002). In the plastics industry, mica is added to adjust volume or density or reduce production costs. Most importantly, mica is used to change the technical performance of a product, for example to increase strength, increase rigidity, or reduce weight.

The particle shape of the filler influences the performance of a composite product. The shape of mica is characterised by aspect ratio. In the mica industry, aspect ratio is defined as the ratio of particle length to particle thickness. The normal aspect ratio of ground mica is between 20:1 and 40:1 when produced using traditional grinding methods. A high mica aspect ratio improves rigidity and dimensional stability of the plastic matrix (Hohenberger et al, 2002). Special grinding techniques can create high aspect ratio mica (HAR) as high as 200:1. These special grinding techniques increase costs and may result in significant material losses.

Ultra-high aspect ratio mica has been produced using chemical cleavage of the mica plates (Caseri *et al*, 1992). This method involves substituting the potassium ions in the mica minerals with lithium ions. Lithium weakens the attractive forces between the mica silicate layers. The layers are then cleaved by stirring in water. This method requires reaction times of up to 46 hours (Caseri et. al., 1992) and is usually commercially impractical due to reagent costs.

In 1951, Bardet (US Pat 2549880, 1951) described another procedure to chemically cleave mica. In this procedure, mica was heated to 800°C, then immediately quenched with a solution of saturated sodium carbonate. The mixture was then neutralised with hydrochloric acid. Caseri explains that sodium and carbonate ions penetrate into the potassium interlayers. When the hydrochloric acid is added, carbon dioxide gas evolves within the layers. The resulting pressure cleaves the muscovite layers. This mechanism of cleavage is used currently to produce mica paper.

Another method that has been used to improve the grindability of ores is microwave irradiation. Microwave assisted grinding has been successfully demonstrated on many different minerals and chemicals. Some minerals, such as lead sulphide, for example, can reach temperatures in excess of 400°C in a less than one minute in a microwave oven

(Kingman et al 2000). However, microwave energy alone has no effect on muscovite mica (Chen et al 1984). The muscovite crystals are transparent to microwave irradiation.

A more efficient approach to produce high aspect ratio mica may involve the use of microwave energy in combination with chemical pre-treatment. The possibility exists that water, or an ion solution, may be introduced between the mica's silicate layers using hydrochloric acid or lithium nitrate solution. Heating the hydrated mica rapidly in a microwave may cause the solution to vaporise within the mica layers. The vapour pressure of the steam may cause the mica layers to delaminate along the cleavage planes. This may result in an increase in the mica aspect ratio.

2 Background

2.1 Introduction

This section describes the physical and chemical properties of muscovite mica. Following this description is a discussion on the uses of mica in industry and world-wide production statistics. Finally, descriptions of current muscovite mining and mineral processing techniques are detailed.

2.2 Physical Properties of Muscovite

Mica is grouped into 37 phyllosilicate minerals (Hedrick, 2003). The term phyllo is derived from the Greek word “phyllon”, or leaf. Mica comes from the Latin word “micare” meaning to shine or flash. Muscovite mica is a plate-like mineral that has unique physical properties. The crystalline structure of mica is formed in layers. These layers can be split or delaminated into large thin sheets. These sheets are chemically inert, flexible, elastic, reflective, and transparent to opaque (Hedrick 2002).

Table 1 describes the physical properties of muscovite mica. Note that mica’s perfect cleavage in the {001} direction, along with a low fracture rate across the crystals, produces a high aspect ratio.

Table 1. Physical properties of muscovite mica (Gaines et al, 1997)

Chemistry	$KAl_2(AlSi_3O_{10})(F, OH)_2$; potassium aluminium silicate hydroxide fluoride
Class	Silicates
Subclass	Phyllosilicates
Group	Micas
Colour	Colourless, white, yellow, silver, green, or brown
Hardness	2.5 to 3.5
Avg. Specific Gravity	2.77 to 2.88
Lustre	Vitreous to pearly
Transparency	Transparent to translucent
Cleavage	Perfect in one direction {001}; sheets or flakes with elastic quality
Fracture	Uneven; rarely observed due to perfect cleavage
Streak	White
Crystal System	Monoclinic; 2/m; several polytypes $2M_1$, 1M, 3T; $2M_2$ common with space group C2/c
Crystal Habits	Distinct crystals rare; tabular with prominent faces {001}; can have diamond shaped prism faces up to 60 degrees {110} mimicking orthorhombic symmetry; can also have hexagonal appearance {010}; can have penetration twins with {310} at twin axis
Gem Use	None
Field Indicators	Perfect cleavage, colour and associations, elasticity, crystal habit
Associated Minerals	Beryl, tourmaline, quartz, feldspars
Associated Rock Types	Igneous, metamorphic, detrital sedimentary

2.3 Chemical Properties of Muscovite

The chemical composition of muscovite mica varies slightly. An example of Norwegian Tuftane and Brazil Lake muscovite can be seen in Table 2. Note that silica, alumina, and potassium oxide are the major constituents. The feed material used for this experiment, Brazil Lake muscovite, has relatively low Fe_2O_3 concentration.

Table 2. Composition of Norwegian Muscovite Mica (Kalinowski et al, 1996) and Brazil Lake Muscovite Mica

	Norwegian Tuftane Muscovite	Brazil Lake Muscovite
SiO_2	47.29	48.11
Al_2O_3	33.74	40.56
Fe_2O_3	4.10	0.49
FeO	1.33	NA
MnO	0.38	0.30
MgO	0.20	0.01
CaO	0.02	0.01
Na_2O	0.60	0.81
K_2O	10.91	10.37
TiO_2	0.21	<0.01
F	0.20	NA
Total	98.98	100.66

Muscovite mica's platy structure consists of two sheets of SiO_4^{4-} tetrahedra arranged in pairs, Figure 1. These tetrahedral sheets enclose an octahedral layer of alumina in a sandwich-like manner. Approximately one of every four silicon atoms in the tetrahedral layer is replaced by aluminium. This substitution of aluminium (Al^{3+}) for silicon (Si^{4+}) results in an overall negative charge in the tetrahedral layer. Large cations, such as

potassium, compensate for the negative charge in the tetrahedral layer and reside between the “sandwich” layers. The mica crystal can be cleaved or split along this potassium interlayer (Hedrick et al 2003).

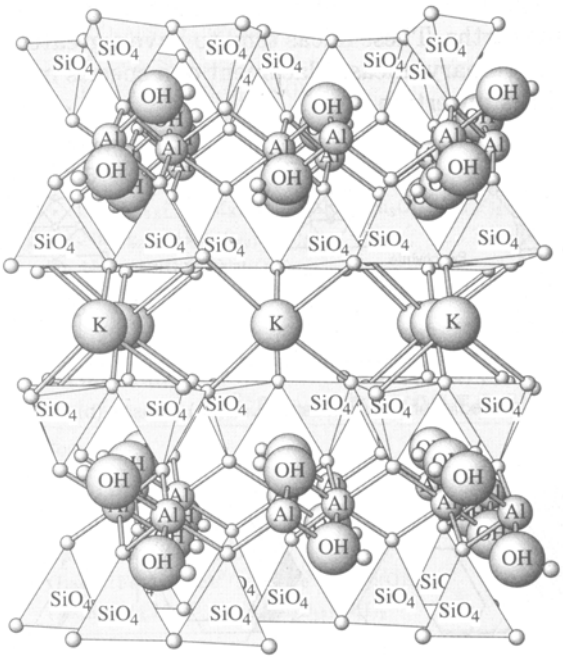

Figure 1. The structure of muscovite mica (Gaines et al 1997)

2.4 Uses of Mica

Mica’s unique properties allow it to be used in various ways in industry. For example, sheet mica has exceptional insulating properties that allow for specialised electrical applications. In other electrical uses, dry ground mica and flake mica can be used to form built-up mica, mica paper, and glass bonded mica. However, more than half of the mica consumed in the United States is in the form of filler material (Hedrick 2002).

There are generally two types of fillers, inactive and active. Inactive fillers are used to reduce costs and are referred to as extender fillers. Active fillers are functional fillers and are used to effect a change in the properties of the compound. For example active fillers can change the surface, colour, density, shrinkage, expansion coefficient, conductivity, permeability, mechanical properties or the thermal properties of a product (Hohenberger et al 2002).

2.4.1 Mica Use in Industry

Applications for commercial mica use are diverse. Mica is used as an active filler in paint. The platy structure reinforces the paint film during drying and curing. Mica increases the paint film flexibility. As the film ages, mica reduces internal stresses resulting from oxidation, thermal expansion, and contraction. Mica in water based paint offers better adhesion and improves weathering. In the automotive industry, wet ground mica imparts a metallic finish to paint (Hedrick 2002).

In the construction industry, mica is also used as an active filler. It acts as an extender in joint compound. The mica also improves the workability of the compound. The platy structure produces a smooth consistency in the finished product, and prevents cracking in the plaster joints.

Mica is used in rolled roofing and asphalt shingles. The mica is applied to the asphalt surface to prevent adjacent surfaces from sticking.

Mica is also used as an additive in the well drilling industry. The ground mica helps to prevent loss of circulation in the drill hole by sealing porous sections in the rock and soil (Hedrick 2002).

Sheet mica has insulating properties that makes it suitable for electrical and thermal applications. The mica is moulded into tubes and rings and is then used as insulators in

transformers, armatures, and motor starters. Mica has a hardness index of 2.5-3.5 (Gaines et al, 1997). The relatively soft nature of mica allows it to be cut or die-punched into many different shapes, such as insulated washers, discs, or cores.

High quality wet ground mica is used in cosmetics. Its natural sheen and lustre make it an important component in nail polish, blush, eyeliner, and foundation (Hedrick 2002). Muscovite mica is non-carcinogenic, non-toxic, and safe for sensitive skin. Mica adheres well to the skin and is able to block ultraviolet light, making it useful in preventing skin cancer. (http://azco.com/mica/micainfo.php)

Dry ground mica is an active filler in plastics. Its plate-like structure improves rigidity and dimensional stability in the filler matrix. In automobiles, mica plastic is used to produce lightweight parts that reduce noise and vibration (Hedrick 2002).

> "Aspect ratio is a very important characteristic of mica products because it has a significant effect on the increase in flexural modulus obtained with a given loading level of mica. High-aspect ratio mica produces the largest increase in flexural modulus". (http://azco.com/mica/micainfo.php)

A summary of typical uses of mica can be seen in Table 3.

Table 3. Typical uses of mica (Skillen 1992)

Grade	Sieve Size (mesh)	Typical Uses
Coarse flakes	6	Oil well drilling, artificial snow
Med-coarse flakes	10	Christmas ornaments, display material
Fine-coarse flakes	16	Concrete block fillers, refractory bricks, gypsum boards, asphalt roofing felts, shingles
Coarse-fine powder	30	Metal annealing, absorbent in explosives, disinfectants, automotive components
Med-fine powder	60	Welding electrodes, cables & wires, foundry works, pipeline enamels, mastics, lubricants, adhesives
Fine powder	100	Texture paints, acoustical plasters, ceiling tiles
Superfine powder	325	Paints, plastics, rubber products, paper

Table 4 indicates volume of mica produced and where it is used in industry in the United States in 2001 and 2002.

Table 4. Ground mica sold or used in the United States [1,2] (Hedrick 2002)

	2001			2002		
	Quantity (thousand metric tons)	Value (thousands)	Unit value	Quantity (thousand metric tons)	Value (thousands)	Unit value
End use:						
Joint cement	46	$8,100	$178	58	$10,600	$183
Paint	20	8,030	407	15	3,880	266
Plastics	3	947	290	5	2,270	465
Well-drilling mud	4	422	102	(3)	(3)	209
Other[4]	17	10,600	629	21	12,900	627
Total	89	28,100	314	98	29,400	302
Method of grinding:						
Dry	W	W	147	W	W	180
Wet	W	W	771	W	W	960

W Withheld to avoid disclosing company proprietary data.

[1]Data are rounded to no more than three significant digits; may not add to totals shown.

[2]Domestic and some imported scrap. Low-quality sericite is not included.

[3]Withheld to avoid disclosing company proprietary data. Data is included in "Other."

[4]Includes mica used for molded electrical insulation, roofing, rubber, textile and decorative coatings, welding rods, and miscellaneous.

2.4.2 World Wide Production

There are many producers of mica worldwide. Russia, the United States, and more recently, South Korea, are the top mica producers. Canada is listed as the fourth largest producer in mica from 1998-2002. Table 5 shows worldwide production of mica.

Table 5. Mica world production, by country (taken directly from Hedrick 2002)

(Metric tons)

Country[3]	1998	1999	2000	2001	2002[e]
Argentina, all grades	3,480	3,097	3,100 [e]	2,772 [r]	2,357 [p]
Brazil	4,000	3,000	5,000 [r]	5,000 [r]	5,000
Canada[e]	17,500	17,500	17,500	17,500	17,500
France[e]	10,000	10,000	10,000	10,000	10,000
India:					
Crude	1,489	1,500 [e]	1,500 [e]	1,300	1,500
Scrap and waste	966	1,000 [e]	950 [e]	1,100	2,000
Total	2,455	2,500 [e]	2,450 [e]	2,400	3,500
Iran[4]	1,084	1,425	2,000 [e]	2,000	2,000
Korea, Republic of, all grades	38,459	24,733	65,249	109,339 [r]	100,000
Madagascar, phlogopite	1,232	54	66	90 [r]	45
Malaysia	3,642	3,675	3,835	4,107 [r, 5]	4,200
Mexico, all grades	890	971	1,658 [r]	648 [r]	700
Morocco	600 [e]	210	1,897	-- [r, e]	--
Norway, flake[e]	2,500	2,500	2,500	2,500	2,600
Russia[e]	100,000	100,000	100,000	100,000	100,000
Serbia and Montenegro[e]	150	50	100	100	100
South Africa, ground and scrap	1,558 [r]	1,010	676 [r]	950 [r]	383
Spain[e]	2,500	2,500	2,500	2,500	2,500
Sri Lanka, scrap	2,800	1,425	1,491	1,161 [r]	1,100
Taiwan	7,750	6,966	6,862	9,733	6,595 [5]
United States, scrap and flake[6]	87,000	95,400	101,000	97,800	81,100 [5]
Zimbabwe	1,309	1,300 [e]	-- [r]	-- [r]	--
Grand total	289,000	278,000	328,000	369,000 [r]	340,000

[e]Estimated. [p]Preliminary. [r]Revised. -- Zero.

[1]World totals, U.S. data, and estimated data are rounded to no more than three significant digits; may not add to totals shown.

[2]Table includes data available through May 30, 2003.

[3]In addition to the countries listed, China, Pakistan, Romania, and Sweden are known to produce mica, but available information is inadequate to make reliable estimates of output levels.

[4]Year beginning March 21 of that stated.

[5]Reported figure.

[6]Excludes, if any, U.S. production of low-quality sercite and sheet mica.

Prices paid for mica is dependent on grade, size, and method of grinding. Wet ground mica generally commands a higher price due to the limited and difficult production. Table 6 lists mica prices in the United States.

Table 6. Mica prices in the United States (Harben 1999)

Product		Price (US dollars)
FOB Plant:	Dry Ground	$190-250/t
	Wet Ground	$600-1300/t
	Micronized	$600-900/t
	Flake	$250-450/t
	Sheet Muscovite Mica	$41/kg
	Splittings	$1.51/kg
N. Carolina:	Flake	$79/t
	Dry Ground	$176/t
	Wet Ground	$1080/t

2.5 Current Mining and Mineral Processing Methods

2.5.1 Introduction

There are two methods used world wide to mine mica. The first method involves the mining of sheet and flake mica that range from 2.5 cm to several meters in diameter. In the second method, mica is concentrated as a secondary product when mining other minerals, such as spodumene, quartz, and feldspar.

Scrap and flake mica produced from circuits such as Figure 2 or Figure 3 are processed further by using wet or dry grinding techniques. These techniques are described in more detail in the following sections.

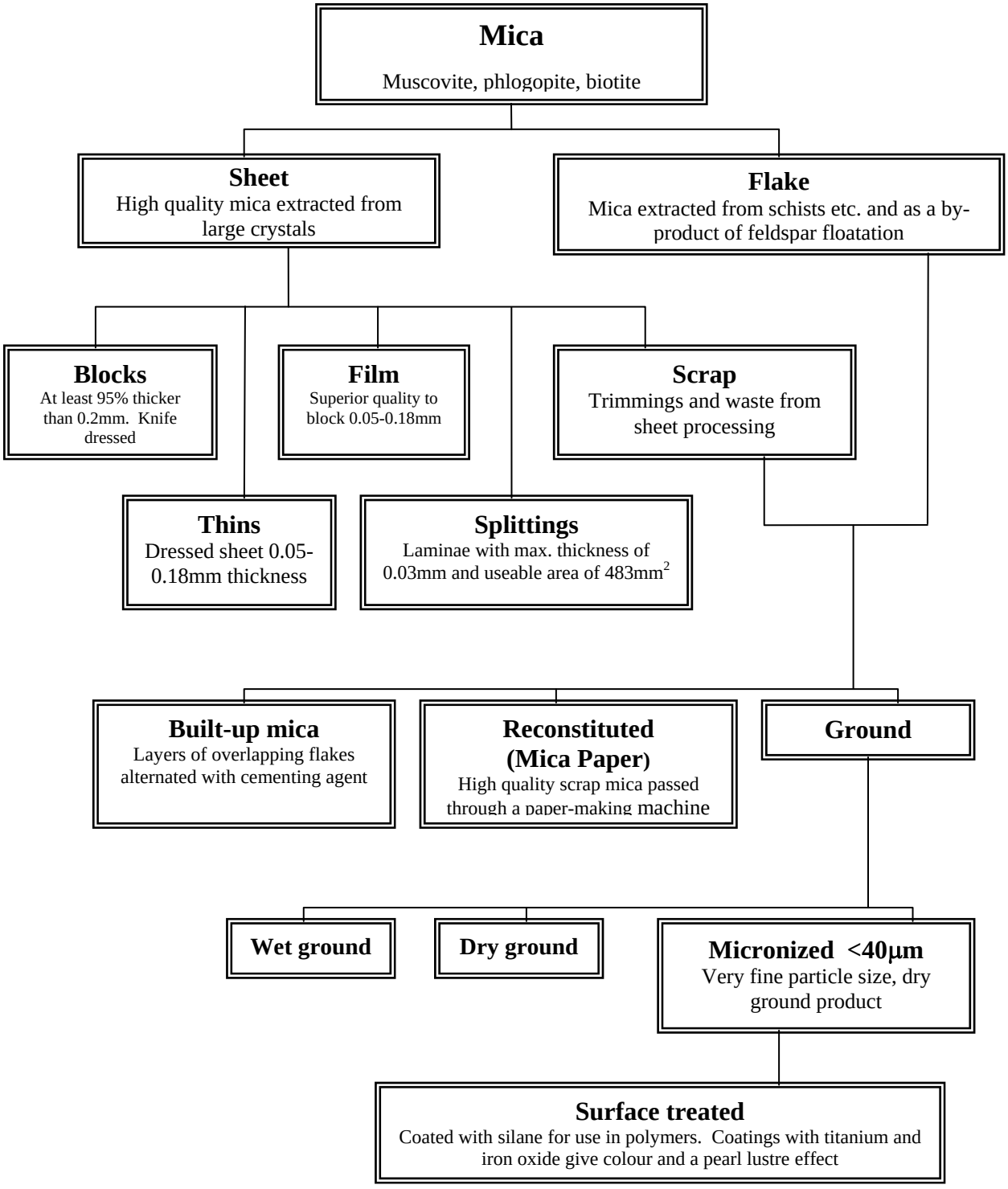

Figure 2. Muscovite processing flow sheet (adapted from Sims 1997)

2.5.2 Sheet and Flake Mica Mining

Sheet and flake mica, from Figure 2, is mined using open pit or underground techniques. Open pit is more common, with the weathered ore being removed with shovels, scrapers, or front-end loaders. The larger pieces are hand picked, while screens are used to separate the smaller flakes. Low velocity dynamite is used to prevent excessive damage to the larger sheets (Harben 1999).

Scrap mica is created during the processing of sheet mica. It is one of the primary sources of feedstock for ground mica. Bench scrap is formed from the crude processing of mined mica blocks, while factory scrap mica is collected during downstream fabrication processes of electrical insulation components (Skillen 1992)

2.5.3 Mica Floatation as a Secondary Product

The second mining method is used with hard granites and pegmatite ores. Mica is collected as a secondary product to the primary feldspar and silica products. The broken ore is crushed using a primary jaw crusher, followed by a secondary gyratory crusher. The gyratory crusher is usually in closed circuit with a screen. A tertiary rod mill in closed circuit with a classifier usually follows, with the final feed product that goes to an acid floatation circuit (Harben 1999). A simplified crushing and mineral processing circuit is shown in Figure 3.

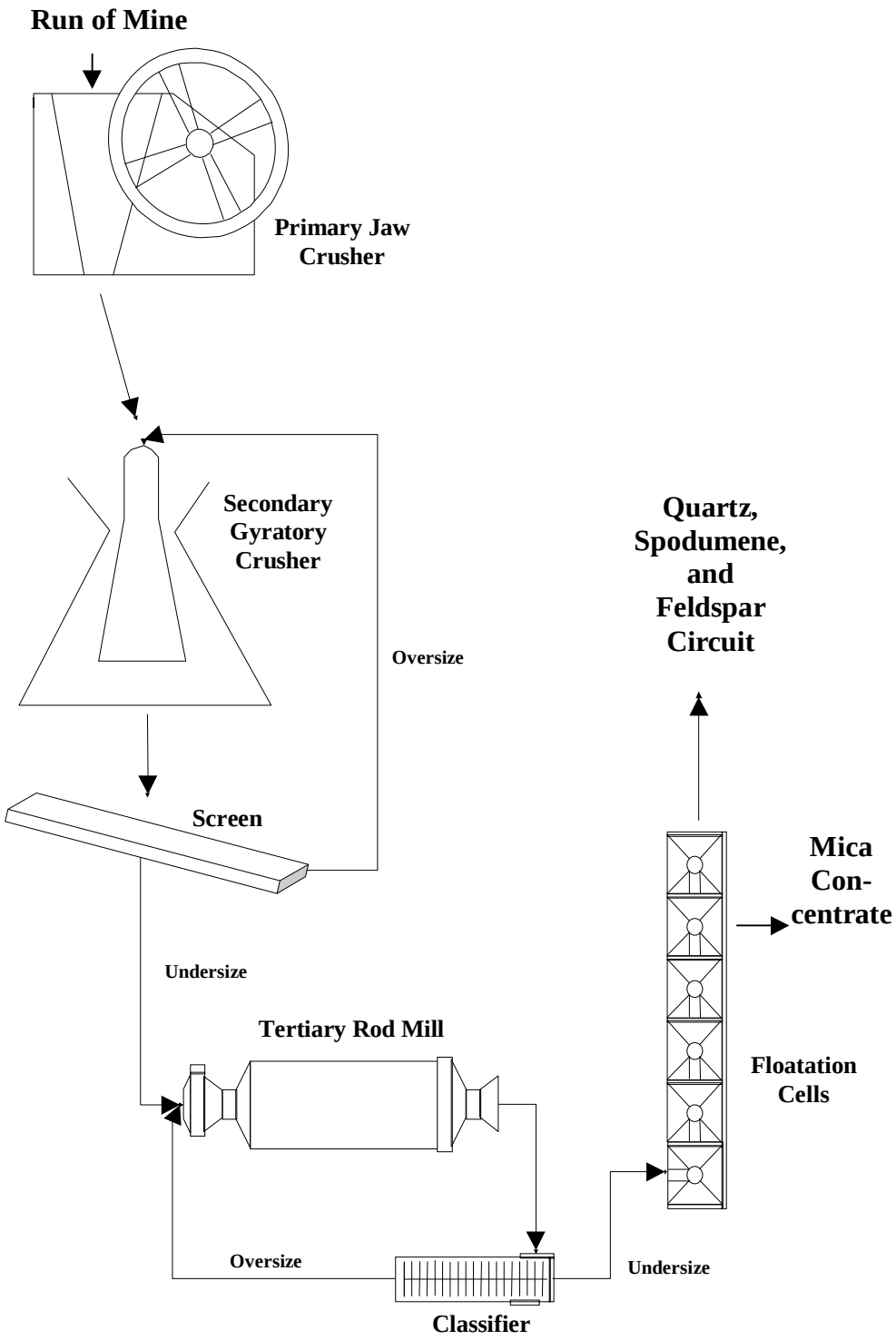

Figure 3. Simplified mica circuit

2.5.4 Mica Grinding Techniques

2.5.4.1 Introduction

Once the mica has been concentrated into a relatively pure form, it is either dry or wet ground. The method of grinding depends on the end use of the product.

2.5.4.2 Dry Ground Mica

When aspect ratio is not as critical for strength, such as in decorations, non-stick backings, joint compounds, well-drilling additives, and welding rods, mica is dry ground using high-speed hammer mills or rod mills. This method produces a coarser ground product. Dry grinding methods produce mica with an aspect ratio of 20 to 40 (Hohenberger et al 2002). According to Kauffman (Kauffman et al 1974), wet or dry ground mica does not produce appreciable amounts of mica with aspect ratios above 30. The ground products are then classified using screens or air classifiers (Harben 1999), and separated by size and aspect ratio.

2.5.4.3 Wet Ground Mica

Wet grinding helps to preserve the aspect ratio of the mica while reducing the size of the particles. In addition, wet grinding imparts higher sheen in the particles, making them an important additive to cosmetics and metallic paints. Wet grinding improves slip in mica, allowing mica to be a substitution for graphite in lubricants (Harben 1999).

Chaser-type or edge-runner mills and Muller mills (Figure 4 and Figure 5) are examples of mills used for wet grinding. Feedstock for wet ground mica is mostly flake mica concentrates that is mixed into a slurry with 25%-35% water, by weight. The output from wet grinding is much lower than that of dry grinding, often less than one tonne per

day per grinding unit. This lower output is reflected in the higher price for wet ground mica, as seen in Table 6.

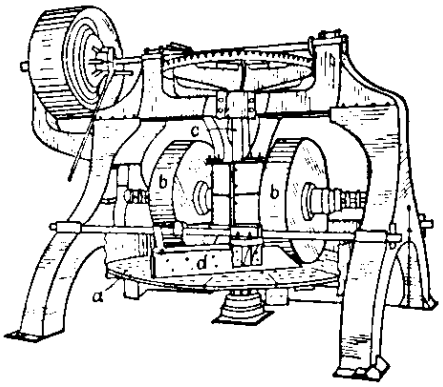

Figure 4. Chaser mill (Taggart 1950)

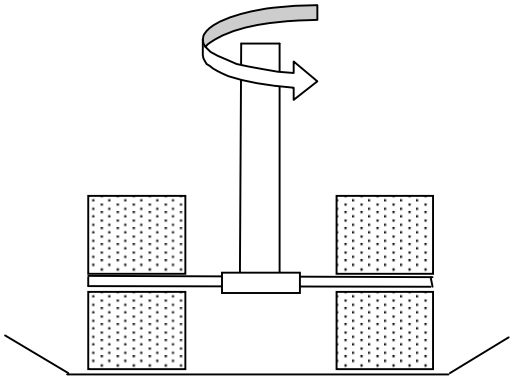

Figure 5. Muller mill

2.5.5 Micronized Mica

Fluid energy mills are used to produce a very fine grade of mica called micronized mica. This material is typically less than 53μm in size. Some suppliers produce material of a size less than 20 microns. Vertical ball mills, opposed jet mills, and spiral jet mills are used to produce micronized mica (Hohenberger et al, 2002).

Vertical ball mills use grinding "pearls" to grind and delaminate the mica. Grinding pearls can be ceramic or metallic. Their small size, usually a few millimetres, produces a large surface area for grinding the mica.

The feed can be wet or dry, and the grinding action results from shear forces between the mica and grinding media. This system can be used in a continuous or batch process (Hohenberger et al, 2002). A simplified diagram of a vertical ball mill is shown in Figure 6.

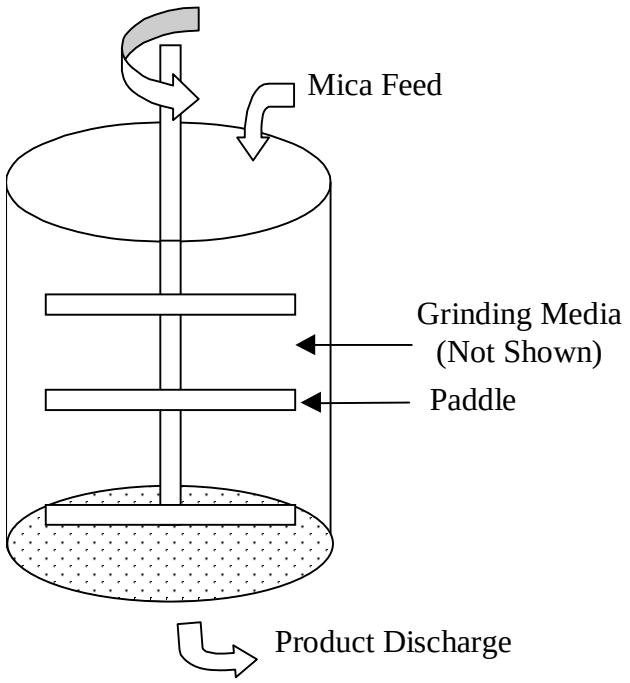

Figure 6. Simplified vertical ball mill

In impact jet mills, particles are fed into compressed air streams and exit through jet nozzles in a vertical chamber. The opposed nozzles can be paired in groups of two or four, and are aligned so that the particles impact each other in the centre of the chamber. An upward movement of air carries the ground material out of the chamber to a classification unit, where coarse and fine particles are separated. These mills are very efficient at reducing particles to micron size. There is no contamination from grinding media, since the particles are broken against each other. However, this type of collision can cause laminar particles to be damaged, reducing the aspect ratio (Hohenberger et al, 2002). A simplified diagram of the opposed jet mill can be seen in Figure 7.

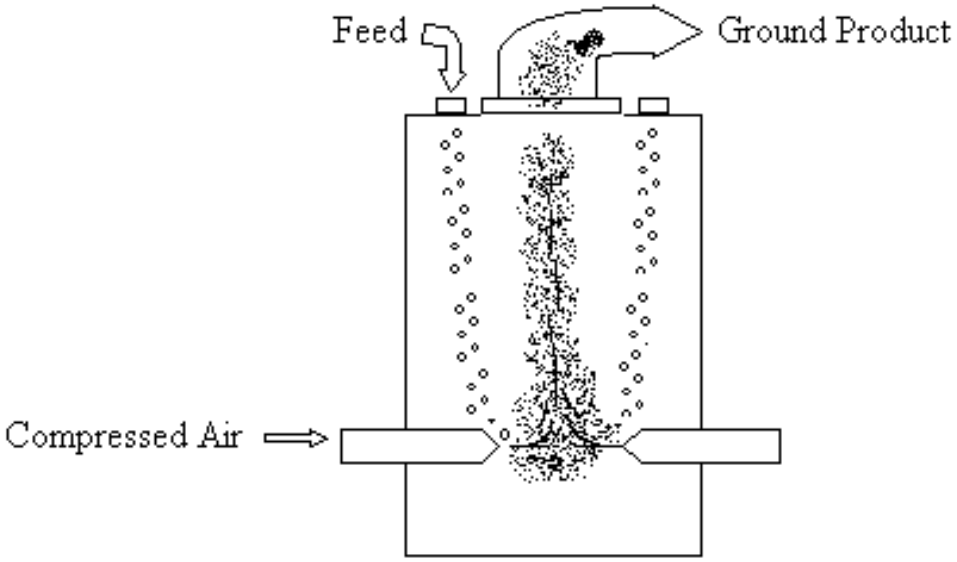

Figure 7. Simplified opposed jet mill

Spiral jet mills have been developed recently, and have some advantages over the impact jet mill. The coarse particles are fed into the grinding chamber via a screw conveyer. Air nozzles are tangentially placed to direct airflow in a high velocity spiral around the chamber. The particles are delaminated by high shear forces generated by the air stream. According to Hohenberger (Hohenberger et al, 2002), mica particles ground in the spiral jet mill maintain a high aspect ratio. The general principle of spiral grinding is seen in Figure 8. The shear forces cause the mica to delaminate without breaking the flakes across the mica grain, thus maintaining a high aspect ratio.

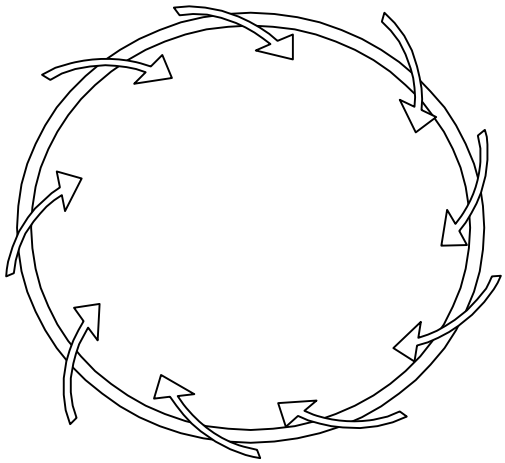

Figure 8. Spiral jet mill

2.6 Microwaves and Mica

2.6.1 Principles of Microwave Heating

Microwave energy is electromagnetic radiation operating at certain frequencies that interacts with dielectric materials to produce heat. Electromagnetic waves contain both electric and magnetic field components (Galema 1997). Dielectric molecules such as water have a positive and negative pole. An oscillating electromagnetic field will cause the water dipole to continuously reorient or rotate (Figure 9). If the frequency is too low, the molecules will move in time with the changing electric field. This will cause little or no heating effect. If the frequency is too high, the water molecules will not have time to reorient, and no heating will occur. At the optimum frequency, operating at 2450 MHz, the water molecules will lag behind the oscillating field (Martin Chaplin 2008). This phase lag results in molecular collisions and an energy loss in the material, resulting in a heating effect (Bradshaw 1999).

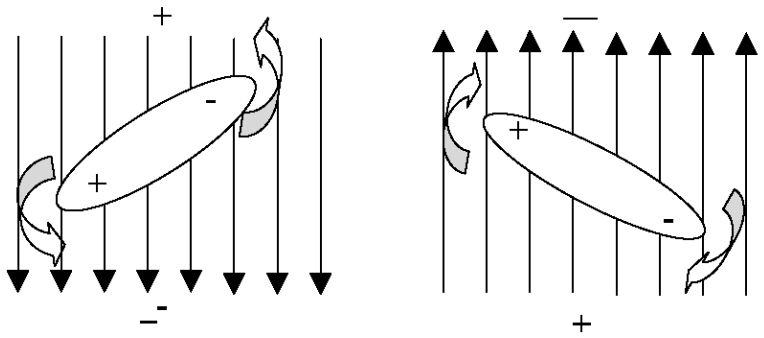

Figure 9. Realignment of a dipole (Al-Harahsheh et al 2004)

2.6.2 Microwave Use in Mineral Processing

Interest in the thermal pre-treatment of ores originates from the need to improve the efficiency of communition and liberation of minerals (Orumwense et al 2004). Walkiewicz et al (1991) state that 50% to 70% of energy used in a mineral processing operation is used for grinding. These authors say that a conventional grinding operation is about 1% efficient. In one example in their experiments on iron ore, microwave preheating improved the grinding efficiency to between 9.9% to 23.9%.

Research has been conducted into how various minerals respond to microwave energy. Minerals can be classified into three principal groups according to how they respond to microwave energy (Al-Harahsheh *et al* 2004). These groups are as follows:

1. Transparent or low loss materials where microwaves pass through with no losses
2. Conductors that reflect microwaves with no penetration
3. Absorbing or high loss materials that dissipate microwave energy as heat

Chen et al (1984) conducted tests on 40 different minerals. Walkiewicz et al (1988) conducted heating tests on 135 reagent grade chemicals and 19 minerals. It was found that generally darker ore minerals heated readily and that silicate gangue minerals heated poorly.

Microwave technology has potential advantages in mineral processing. Microwaves can be used in thermally assisted grinding of many ores (Kingman et al 2000). Different minerals have varying degrees of thermal resistance. Minerals that heat rapidly in the presence of microwave energy encounter expansion or transformation relative to the surrounding gangue material. It is thought that this differential thermal expansion strains or weakens mineral grain boundaries, and facilitates the creation of intergranular fractures (Walkiewicz et al 1991). A significant implication of selectively heating certain minerals is in energy savings. Only the mineral of interest needs to be heated, and not the gangue material.

Research has been conducted in the field of microwave assisted leaching. Al-Harahsheh et al (2004) described how research in this field has demonstrated increased recoveries in the leaching of copper, zinc, nickel, and refractory gold ores.

2.6.3 Effect of Microwave Irradiation of Muscovite Mica

Chen et al (1984) have indicated that muscovite is transparent to microwave irradiation at 2450 MHz. In fact, the authors found that most silicates, carbonates, and sulphates, are transparent to microwave energy, Table 7.

Table 7. Minerals transparent to microwave irradiation (Chen et al 1984)

Mineral Class	Minerals/Compounds
Carbonates	Aragonite, calcite, dolomite, siderite
Jarosite-type compounds	Argentojarosite, synthetic natrojarosite, synthetic plumbojarosite
Silicates	Almandine, allanite, anorthite, gadolinite, muscovite, potassium feldspar, quartz, titanite, zircon
Sulphates	Barite, gypsum
Others	Fergusonite, monazite, sphalerite (low-Fe), stibnite

Water, however, is easily heated by microwave irradiation at 2450 MHz. The fundamental importance of this statement to this experiment is the following concept: If one could introduce water between the interlayers of the mica, the mica could then be irradiated with microwave energy, and the water within the interlayer would be heated. This heat might cause the water to vaporise. The pressure of the water vapour may force the silicate layers apart, or at the very least, may start to open the layers near the edge of the mineral grains. A similar cleavage mechanism as described above is used in the Bardet process. This process is used to produce partially exfoliated mica for the manufacture of reconstituted mica paper.

2.7 Chemical Delamination Processes

2.7.1 The Bardet Process

This process was patented by J. J. Bardet (Bardet,1951). Bardet describes how muscovite can be cleaved using saturated Na_2CO_3 solution and HCl acid. The mica is heated to 800°C, quenched in the Na_2CO_3 solution and neutralised with HCl. The mixture is then stirred to complete the delamination. This procedure is used commercially and can produce surface areas of 2-5 m^2/g of mica (Caseri et al 1992).

Caseri (1992) explains that the sodium and carbonate ions penetrate into the potassium interlayers. When the HCl is added, CO_2 gas evolves and the gas pressure causes the mica layers to cleave.

2.7.2 The Caseri Process

Caseri (1992)uses a chemical process in his experiments to delaminate the mica flakes. Caseri's procedure allows the potassium interlayers to become hydrated, and thus more easily delaminated.

The Caseri (1992) process produces high aspect ratio muscovite mica using a chemical cleavage process. The mica is treated with a concentrated lithium nitrate solution (65g of $LiNO_3 \cdot xH_2O$ in 25ml of water) in a round bottom flask. The flask is fitted with a reflux condenser and stirred for 46 hours at 130°C. The muscovite is finally washed with water and stirred for 30 minutes before being vacuum filtered, washed, and dried.

The specific surface area of the treated muscovite is measured using methylene blue adsorption. Caseri started with material having a specific surface area of 3.4 m^2/g, while the cleaved muscovite had a specific surface area of 295 m^2/g. Caseri calculated the average thickness of the muscovite plates using a density of 3 g/cm^3 and a basal spacing of about 1.0 nm. The starting material was calculated to be 200 nm thick, and the cleaved muscovite 2-3 nm thick.

Caseri found that the aspect ratio increases with decreasing plate thickness. However, the change in starting aspect ratio and final aspect ratio was not as dramatic as was the change in plate thickness. Caseri found that both the plate thickness and diameter changed in parallel with the treatment, resulting in a moderate increase in aspect ratio.

Caseri used a process that artificially "weathers" the mica. The natural weathering process of minerals in rock and soil is well studied, and is discussed in the following section.

2.8 Weathering of Mica

Artificial "weathering" of muscovite may help in the production of high aspect ratio mica. The natural weathering process involves physical and chemical changes to minerals in soil and rock (Brady 1974). There are several factors that can influence the rate of weathering of mica, including temperature, pH, particle size, and mica type (Fanning and Keramidas, 1977). It may be possible to accelerate the chemical weathering process in muscovite, i.e. artificial weathering, using a lithium nitrate or a hydrochloric acid leach.

The effect of pH on weathering rates in mica has been studied. Kalinowski and Schweda (1996) studied the kinetics of muscovite, phlogopite, and biotite alteration at pH 1 to 4. Their tests were conducted at room temperature. They found that reaction rates increased with decreasing pH. During their tests, they also found that the specific surface area on the micas had increased. The authors noted that "It is conceivable that the increase of surface area during the dissolution of micas is mainly caused by exfoliation of the 2:1 layers". Some of their results are listed in Table 8.

Table 8. Specific surface area measured (Kalinowski et al 1996).

pH	Specific Surface Area m^2/g
	Muscovite
	Unreacted 7.41±0.3
4	9.86±0.3
3	7.16±0.5
2	8.65±0.6
1	13.2±0.2

The increase in surface area by exfoliation in the Kalinowski and Schweda study is explained by hydration. Hydration is one of the chemical processes of weathering in micas. It is the attachment of hydrogen or hydroxyl ions into the crystal lattice of the

mica. The hydrogen and hydroxyl ions migrate along the interlayers between the octahedra and tetrahedra sheets. Once hydrated, the mica crystal is expanded and more porous, making it more susceptible to other decomposition processes (Brady 1974).

Fanning and Keramidas (1977) developed a model supporting this process, as seen in Figure 10. Potassium ions are released from the potassium interlayer as hydrated cations are exchanged. The authors wrote that the potassium interlayers are opened simultaneously along edges and fractures on the mica grains. The interlayers may only be opened partially, at first, giving way to the terms “mica core” and “frayed edge”. In addition, the term “wedge” has been given to the opening of the interlayer where the interlayer meets the mica core.

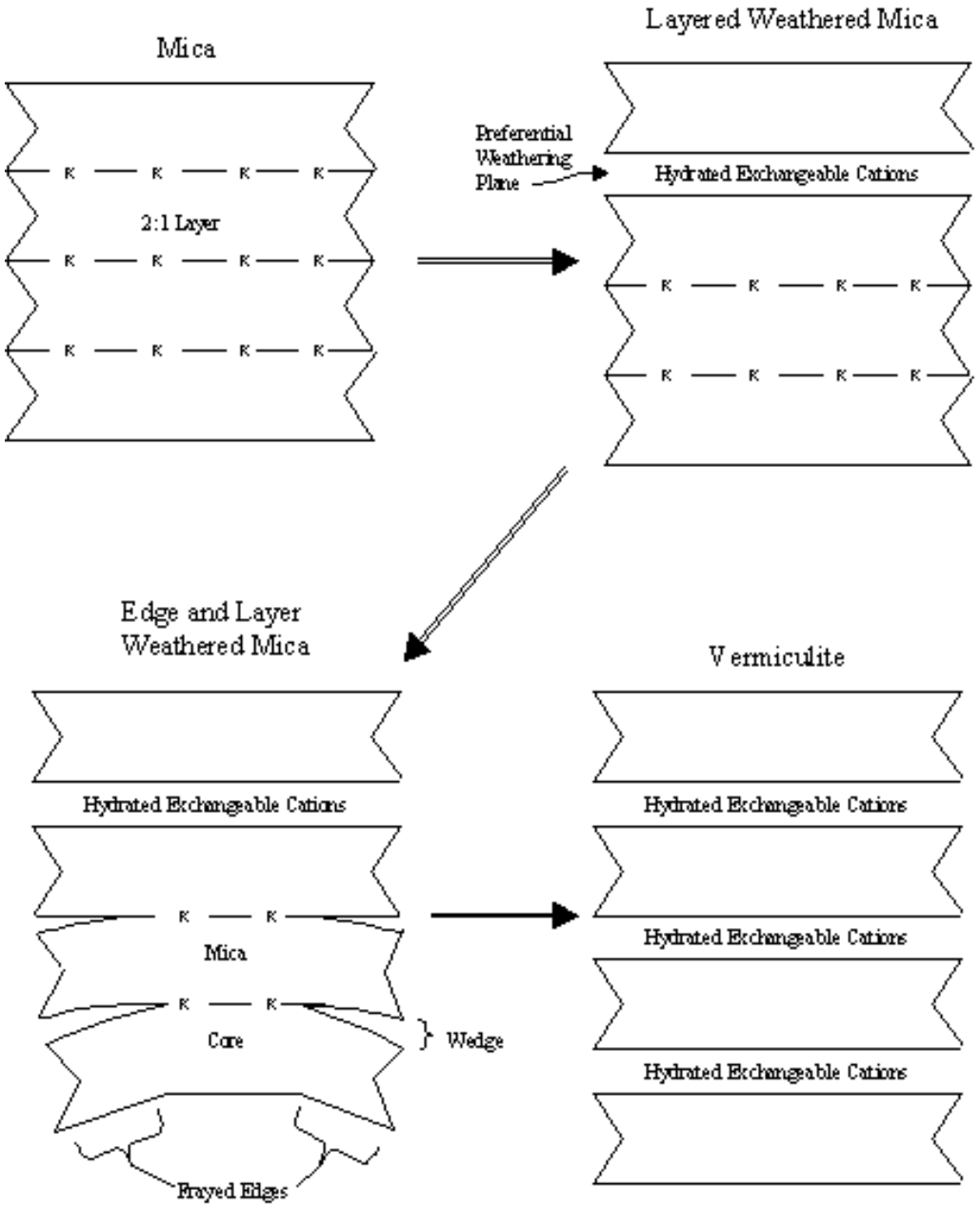

Figure 10. Layer weathering and edge weathering of micas (Fanning et al, 1977)

This model theory has implications for this experiment. The muscovite grains, while still wet from an acid weathering process, could be irradiated with microwave energy. The entrapped water in the wedges and frayed edges might volatilise from the microwave

energy. The volatilised water vapour might exert internal pressure within the hydrated interlayer. This in turn might cause the wedges and partially opened interlayers to open completely delaminating the muscovite grains along the cleavage planes. Delaminating the muscovite mica without changing the length and width of the grains will increase the aspect ratio of the mica grains.

When hydrochloric acid is used to treat the mica the hydrated cation is H_3O^+. The lithium treatment is used to exchange potassium with lithium ions in the mica interlayer. If this exchange is successful hydration of the new lithium interlayer would be more likely (Caseri 1992).

The potassium release at the weathered edges is a diffusion-controlled process, and the rate of potassium release increases with decreasing particle size. Fanning and Keramidas (1977) write, "…smaller mica particles release their K more rapidly than larger particles." This potassium release is an indication of hydration within the interlayers. In addition, the potassium release at the weathered edges is a diffusion-controlled process, and the rate of potassium release increases with decreasing particle size.

A weathered mica powder sample with a smaller particle size distribution should have a greater amount of edge weathering than a coarser weathered powder sample. This overall increase in edge weathering sites should help to maximise the number of "wedges" at the mica edges. This could help delaminate mica grains during the microwave heating.

2.9 Summary

Muscovite mica is mined and processed throughout the world. Mica is used as a functional filler in many applications, such as in joint compound, electrical insulation, and plastics. The single most important feature of mica is high aspect ratio, the ratio of width to thickness. High aspect ratio mica filler is desirable in speciality applications, such as in automotive plastics.

Mica filler is normally processed using wet or dry grinding techniques. These techniques produce mica with an aspect ratio of between 20 and 40. Other processes are used to produce high aspect ratio mica, but are not used commercially to produce large quantities of mica filler for the plastics industry. These processes, Bardet and Caseri, essentially work to delaminate the mica. Bardet uses expanding gas within the interlayers to exfoliate the mica, while Caseri uses cation exchange and hydraulic forces to separate the silicate layers.

Another mechanism that naturally delaminates mica is weathering. Mica weathering is influenced by pH, temperature, and particle size. The weathering process involves cation exchange (hydration) within the potassium interlayer in muscovite mica. This process results in mica that will delaminate along the hydrated interlayer. Frayed edges and wedges will also form at the interlayer edges.

Microwave irradiation operating at 2450 MHz will not affect muscovite directly, but will easily heat water to boiling. With this in mind, treating finely ground muscovite mica with hydrochloric acid or lithium nitrate may induce artificial weathering in the mica grain. This treatment may cause the mica to become hydrated, thus opening or partially opening the interlayers and forming “wedges” at the grain edges. Water may become entrapped in these “wedges”, and when heated in a microwave oven, may volatilise. The

resulting pressure from the water vapour may cause the delamination of the mica grain. Delamination of the mica will increase the aspect ratio.

3 Experimental

3.1 Brazil Lake Muscovite Characterisation

A sample of muscovite mica from the Brazil Lake Pegmatite deposit was obtained. The deposit, located 25 km north of Yarmouth, Nova Scotia, contains approximately 10% muscovite. Both primary and secondary muscovite are present in a 1:4 ratio, i.e. 20% primary and 80% secondary muscovite mica. Primary muscovite formed during the initial crystallisation of the pegmatite. This mica is characterised as 1-2cm diameter euhedral crystals that are unevenly distributed throughout the pegmatite dyke.

The muscovite used for this experiment was secondary muscovite that was formed by a later episode of pegmatite formation. The original potassium feldspars were subjected to sodic alteration. Potassium ions in the feldspar were replaced with sodium ions, providing an excess of potassium in the system. The excess potassium combined with aluminium, oxygen, and silica to form the secondary muscovite. (Black, 2003)

3.2 Materials and Methods

3.2.1 Preparation of Feed Sample

The muscovite mica feed sample was prepared from mica obtained from Champlain Resources, Yarmouth County, Nova Scotia. Approximately 500g of +4mm mica was hand picked to remove impurities, such as silica, feldspar, and other granite host rocks. Figure 11 shows a photograph of the muscovite mica used for this thesis. For the experiment is was necessary to have an homogenized feed sample with a consistent size distribution. Therefore, the mica flakes were ground in a Spex Shatterbox (a ring and

puck pulveriser) to pass through a 100 mesh screen. The ground mica sample was then agitated in a polyethylene bag to ensure homogeneity.

Figure 11. Champlain Resources muscove mica > 4mm

3.2.2 Reagents and Equipment

The equipment and reagents shown in Table 9 were used in this experiment. A description of how they were used follows in the “Procedure” section.

Table 9. Equipment and reagent list

Equipment
Pyrex test tubes 50ml
Rubber stoppers for test tubes
Test tube rack
25 ml graduated cylinder
1 litre beaker
Hotplate
Fume hood
Millipore vacuum filter system
Whatman #4 filter paper - 12.5cm
Petri dishes and covers 100mm
Microwave oven, General Electric Model JM0405-2, 1.0 Kw
Timer, seconds and minutes
Dryer oven, Fisher Isotemp Model 501
Braun coffee grinder, Model KSM2
Plastic vials 50 ml, with sealing snap caps
Balance, Mettler Model PC 440
Weighing paper, Fisherbrand 09-898-12B
Scupula for weighing samples
Spatula for scraping samples
Malvern Laser Particle Size Analyser, Model 2600, PS14A Sampling Module
Hitachi Scanning Electron Microscope, Model S-4700 FEG
Spex Shatterbox, Model 8500
Tyler 100 mesh screen and pan
Reagents
500g muscovite mica <100mesh
Hydrochloric Acid, Concentrated Reagent Grade (38%), A144 P4
Lithium Nitrate, BDH Technical Grade
Distilled Water

3.2.3 Procedure

3.2.3.1 Introduction

The muscovite mica feed sample was ground in a Braun coffee grinder to establish a baseline aspect ratio analysis for comparison with the chemically treated mica. Two leaching experiments were conducted by separately treating the mica feed with concentrated hydrochloric acid (38% w/w HCl), and lithium nitrate solution. A complete flow sheet of the thesis experimental procedure can be seen in Figure 12.

3.2.3.2 Baseline Grind Test

Nine grams of mica feed sample was weighed and placed into the coffee grinder. The sample was ground for two minutes. The top and sides of the coffee grinder were tapped periodically during the grinding to dislodge any material that stuck to the sides of the sample holder. After grinding, the material was removed and placed into a plastic vial. The control grind test was performed in triplicate, and the ground products were labelled GT-1, GT-2, and GT-3.

Material from each of the control grind tests was combined to form a composite sample. The composite sample would serve to “average out” any variances in the grinding procedure. Two grams each of material from GT-1, 2 and 3 were weighed and then placed into a 50-ml plastic vial labelled GT Composite. The sample GT Composite was analysed for particle size distribution and aspect ratio. The results of the analysis served as a baseline for the HCl and lithium nitrate leach tests.

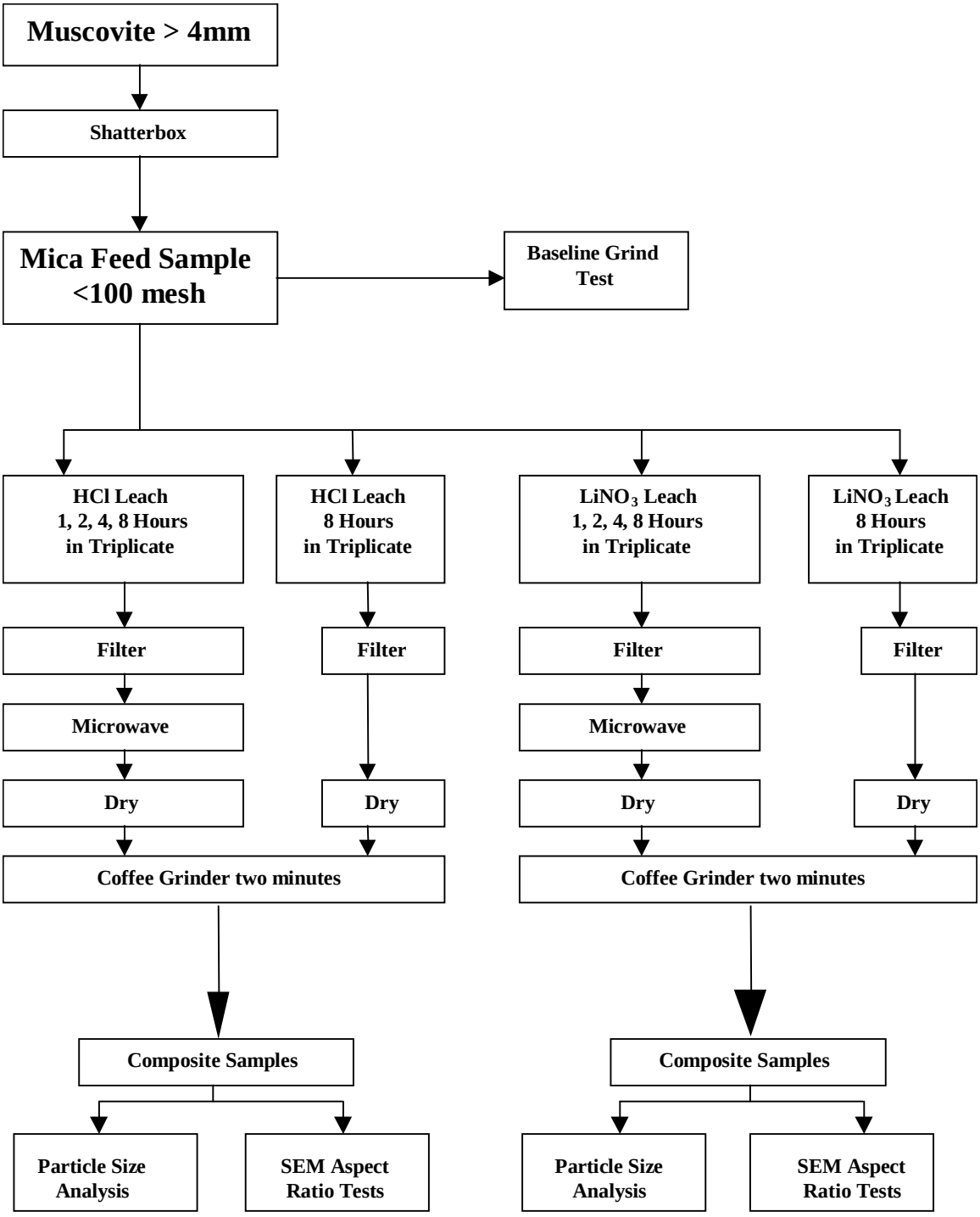

Figure 12. Flow sheet for experimental procedure.

3.2.3.3 Hydrochloric Acid Leach Test

Ten grams each of <100 mesh mica feed sample were weighed into fifteen 50 ml test tubes. Twenty ml of concentrated HCl (38%) was added to each sample. Concentrated HCl was used in order to maximise any pH effect the leaching may have on the mica plates. The test tubes were stoppered and mixed thoroughly. The test tubes were then placed in a water bath at 100°C. The samples were removed from the bath at thirty-minute intervals for mixing. The tests were conducted in triplicate for one, two, four, and eight hours residence time in the hot water bath. Three separate samples were leached for 8 hours to act as a control test. These separate samples were not irradiated with microwave energy.

When removed from the hot water bath, each sample was filtered through a Millipore suction filter using Whatman #4 filter paper. The damp filter paper and residue were then placed into a petri dish and covered. The petri dishes and samples were heated one at a time in a microwave oven on high power. After three minutes they were removed from the microwave. The covers were removed, and the samples were dried in an oven at 110°C for twenty-four hours. The dried samples were then placed in plastic 50ml vials, sealed, and labelled.

Some sample material was lost during the leaching and filtering process due to spillage. This resulted in sample residues with less than the starting weight of ten grams, but more than nine grams. To ensure that all the grind tests were conducted with the same amount of material, nine grams of the dried samples were weighed and placed into the coffee grinder. The samples were ground for two minutes and then transferred into new-labelled 50-ml vials. A composite sample was made from the triplicate tests. For example, two grams each of “HCl 1 Hour GT-1”, “HCl 1 Hour GT-2”, and “HCl 1 Hour GT-3” were weighed and placed in a new vial, labelled “HCl 1 Hour Composite”. This procedure

was repeated for the two, four, and eight-hour leach tests. Particle size distribution tests and aspect ratio measurements were performed on these composite samples.

As a test control, another set of three samples was leached for 8 hours. This set was not irradiated with microwave energy after leaching and filtering. The sample was dried for twenty-four hours and then ground in the coffee mill for two minutes. A composite sample was made by combining two grams of material from each sample. This composite was labelled “HCl Leach 8 Hours – No Microwave”.

3.2.3.4 Lithium Nitrate Leach Test

The same procedure was followed for the HCl leach test, except that the leach solution used was lithium nitrate at 128-g/l concentration. The lithium nitrate solution was kept at a lower concentration than in Caseri’s experiment. This was done to minimise delamination of the mica plates by excess hydration of the potassium interlayer. Excess delamination at this stage would mask any effect the microwave irradiation may have on the mica plates.

The grind test samples were labelled similarly; for example “$LiNO_3$ Leach 1 Hour GT-1”. A control test with no microwave irradiation was performed on the eight-hour leach. A composite sample was made from each triplicate test. These composite samples were used for the particle size distribution analysis and the aspect ratio measurements.

3.3 Analysis for Particle Size

3.3.1 Principle of Laser Diffraction

The Malvern 2600 particle size analyser uses a low power monochromatic beam of light. This visible beam illuminates the particles being measured within a sample cell, and incident light is diffracted by the particles and focused onto a silicon array (Malvern

1986). The diffracted light pattern is stationary, regardless of particle movement in the illuminated sample cell. Figure 13 depicts the principle of laser diffraction (Microtrac Inc., http://www.microtrac.com/laserdiffraction.cfm)

The diffraction pattern is focused onto the silicon array by the Fourier transform lens. The array contains a multi-element photo-electric detector which produces an analogue signal directly proportional to the incident light intensity. The analogue signal is transferred to the computer where the software interprets the diffraction pattern and performs the necessary calculations.

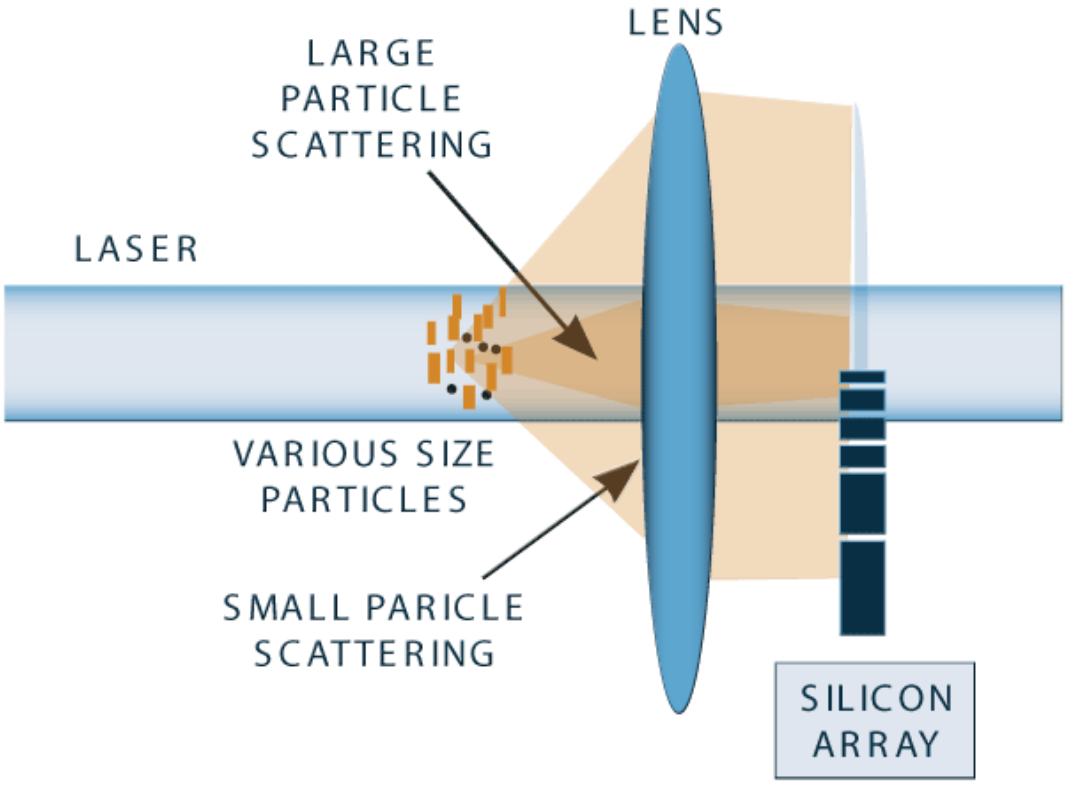

Figure 13. Principle of laser diffraction, Nov 17, 2008 (Microtrac Inc.)

3.3.2 Non-spherical Particle Size Analysis

The Malvern 2600 software calculates size distribution based on spherical dimensions, even though mica particles are plate-like in morphology. Most commercial instruments assume a spherical shape for data analysis (Bowen et al, 2002). Image analysis provides a more accurate method, but is slow and time-consuming.

Bowen et al have found that laser diffraction and image analysis will have "very good" correlation if several assumptions are made. First, the mica discs are assumed to align perpendicularly to the incident light within the measurement cell. Secondly, the diffraction pattern of the disc is assumed to approach that of a sphere. If mica plate edges are presented to the incident light, the signal is significantly weaker and will be masked by the signals from mica plates that are presented to the light. Finally, the image analysis data must be renormalized using the "spherical volume" of the disc, i.e. using the circular diameter and rotating through 180° (rotational volume diameter).

For the purpose of this experiment, the actual or "true" size distribution analysis of the mica particles was not of critical importance. The relative size distributions of the GT baseline grind test, HCl leach, and lithium nitrate leach test are of greater importance. Since grinding parameters were kept constant in the experiments, the laser diffraction method will detect relative changes in size distribution between the tests.

3.4 Analysis for Aspect Ratio

The composite samples were measured for aspect ratio using the Hitachi scanning electron microscope, Model S-4700 FEG. For each sample measurement, a few micrograms of composite sample was placed on copper foil and mounted on a sample holder. The sample holder was tilted and moved in the SEM to provide images that

showed mica grain edges. Up to fifteen images per composite sample were captured using computer software “Quartz PCI v. 5.5” (Quartz Imaging Corporation) . The images were saved and stored for later measurements.

To measure the mica grain thickness, computer software “Quartz PCI v. 5.5” was used. Only mica grain edges that were clearly visible and oriented at or near perpendicular angles were measured. The grain thickness measurements were recorded for each composite sample, and an average thickness was calculated. The test results from the Malvern particle size analyser were used to provide a mean particle diameter for each composite sample. This mean diameter was used in the calculation of aspect ratio, the average particle width divided by the average particle thickness.

4 Results

4.1 Particle Size Distribution

4.1.1 Feed Sample and Baseline Grind Test

The particle size distribution (PSD) of the mica feed sample was determined using the Malvern particle size analyser. The particle size distribution of the composite ground feed sample was also determined. Estimated standard deviation of the d_{50} value is 2.0. The feed sample mean particle size, or d_{50}, was 71.9 microns. The mean volume diameter, or d(4,3), can be seen in Appendix A in Table 16. The particle size distribution of the composite grind test was found to have a d_{50} of 43.0 microns. Figure 14 shows a graph of the particle size distribution of the feed sample <100 mesh and the size distribution of the ground feed sample.

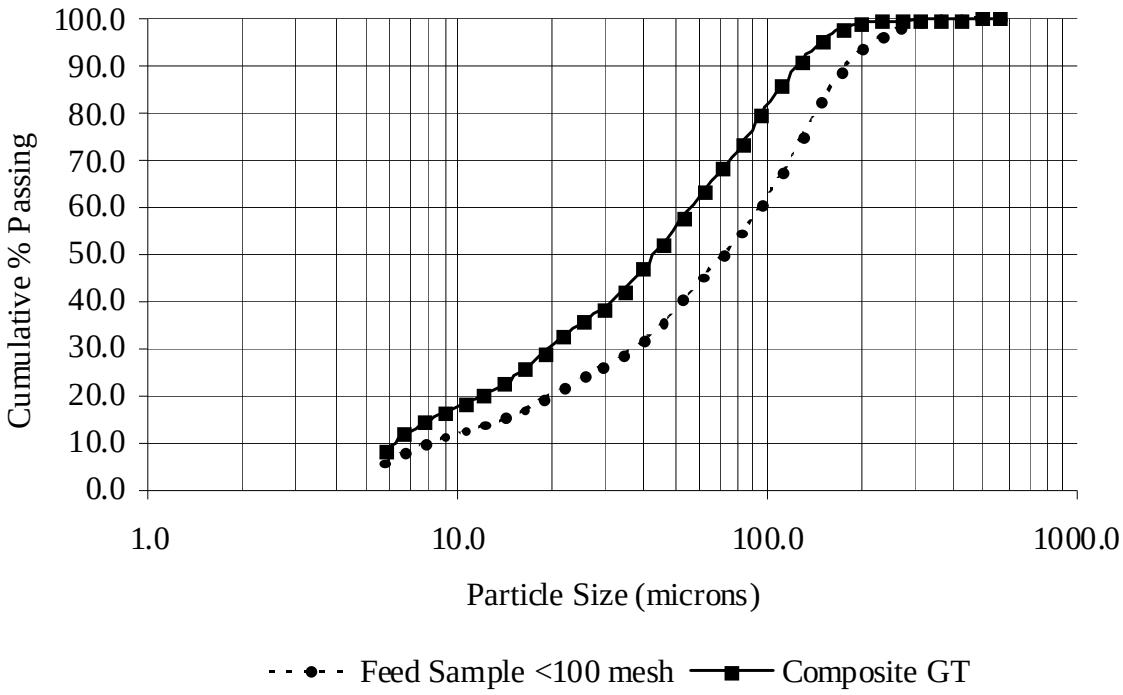

Figure 14. Particle size distribution of mica feed and GT composite sample.

4.1.2 Hydrochloric Acid Leach

In Figure 15, the particle size distribution of the HCl leached, microwave irradiated and ground mica is displayed. The d_{50} or average particle sizes for the 1, 2, 4, and 8-hour leach times were 42.5, 42.9, 41.5, and 47.1 microns, respectively. Estimated standard deviation of the d_{50} value is 2.0.

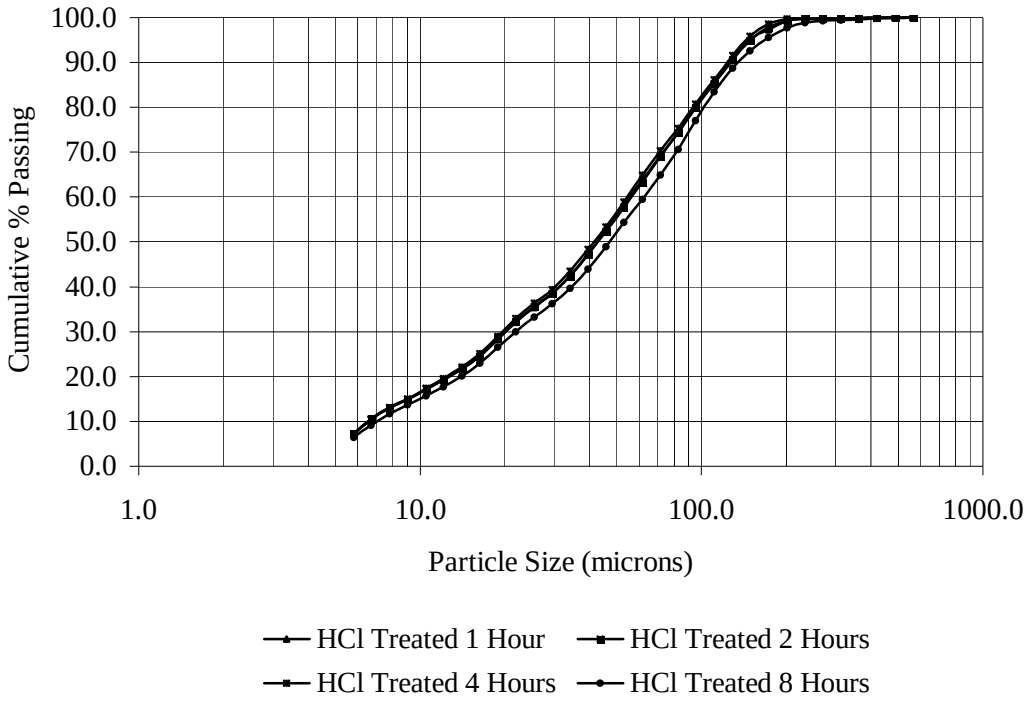

Figure 15. PSD of HCl leached mica, with microwave irradiation and grinding.

A control test was performed to determine if the microwave irradiation was having any effect on the mica. The HCl 8-hour leach test was repeated, but the filter residue was not treated with microwave irradiation. It was thought that the 8-hour HCl leach would demonstrate the largest difference in particle size distribution between the microwave

irradiated and non-irradiated tests. The d_{50} for the HCl 8-hour leach test was 47.1 μm, while the d_{50} for the HCl 8-hour control test was 49.9 μm. Estimated standard deviation of the d_{50} value is 2.0. A graph of the particle size distributions can be seen in Figure 16.

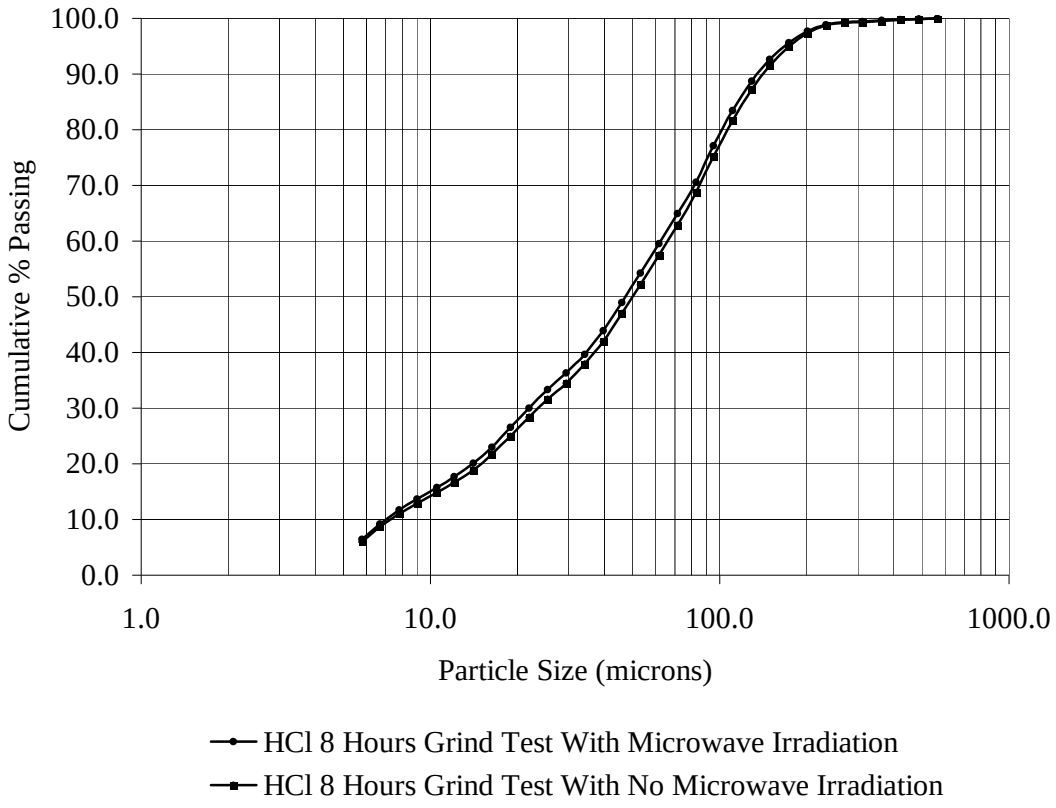

Figure 16. Particle size distribution comparing 8-hour HCl leach with and without microwave irradiation, followed by grinding.

4.1.3 Lithium Nitrate Leach

The mica feed sample was leached in lithium nitrate solution for 1, 2, 4, and 8 hours. The results of the size analysis can be seen in Figure 17. The d_{50} values are 45.4, 45.1, 46.8, and 46.1 microns, respectively. Estimated standard deviation of the d_{50} value is 2.0.

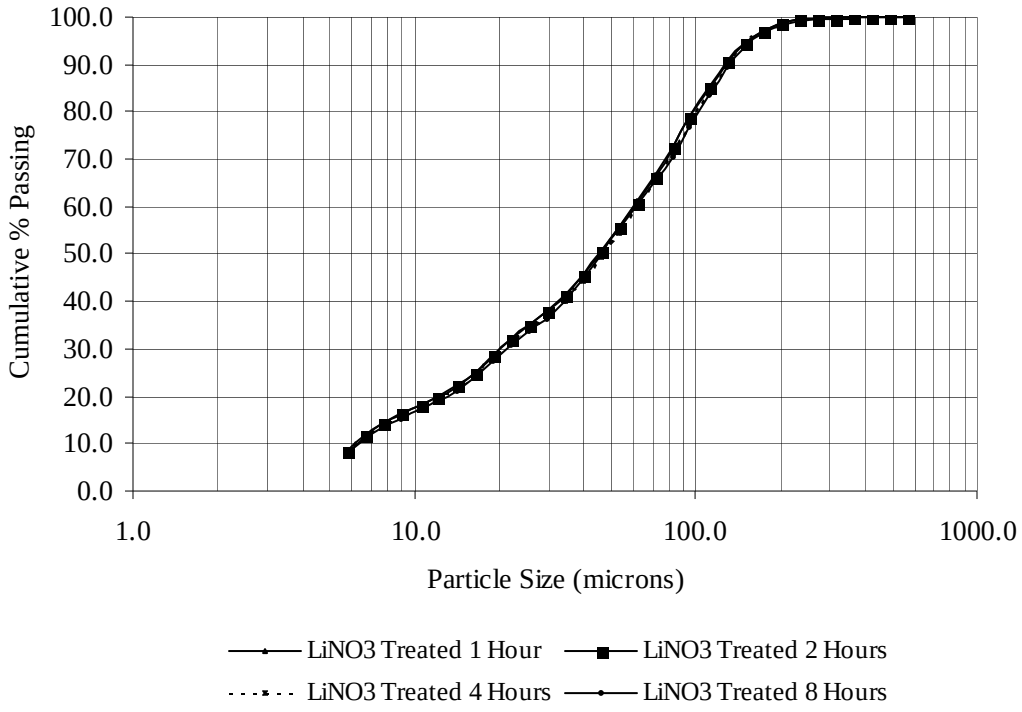

Figure 17. Particle side distribution of lithium nitrate leached mica, with microwave irradiation and grinding.

A control test was also performed for the lithium nitrate leach. This test was done in the same manner as in the HCl leach control test, see previous section above. The 8-hour leach with microwave irradiation resulted in a d_{50} of 46.1 microns, while the 8-hour leach with no microwave irradiation had a d_{50} of 48.3 microns. Estimated standard deviation of the d_{50} value is 2.0. A graph of the particle size distributions can be seen in Figure 18.

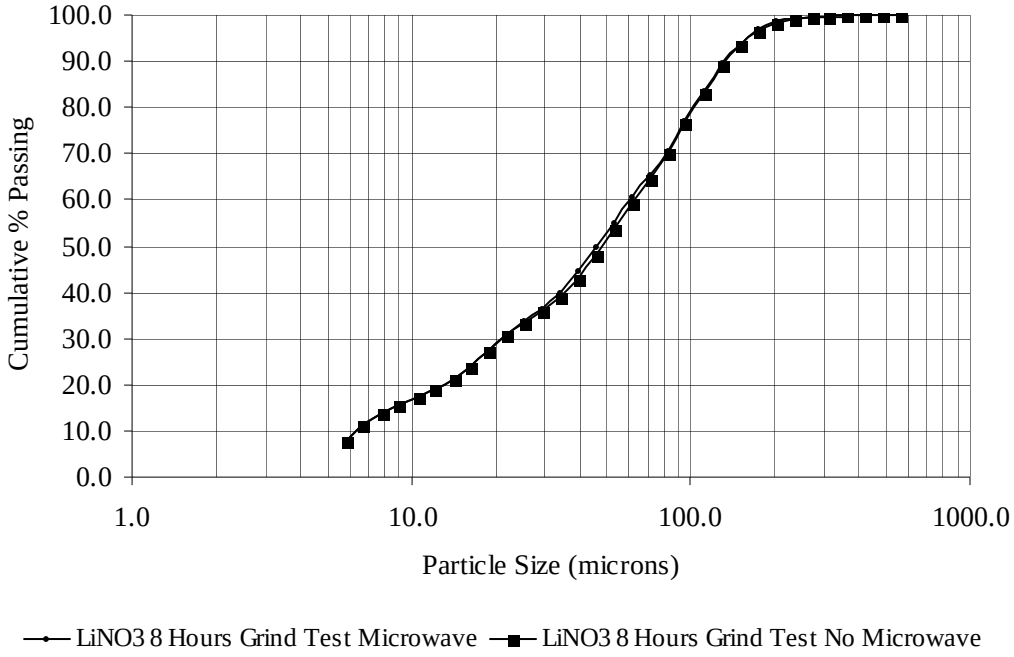

Figure 18. PSD comparing 8-hour lithium nitrate leach with and without microwave irradiation, followed by grinding.

4.2 Muscovite Thickness Measurements

4.2.1 Introduction

The muscovite samples, feed sample <100 mesh and Baseline Grind Test, were examined using the Hitachi scanning electron microscope (SEM). The hydrochloric acid leach series and the lithium nitrate leach series were also examined using the SEM.

The images from the SEM were captured and saved using Quartz 5.5 computer software. The image analysis was also performed using Quartz 5.5. Each image contained a scale measured in microns. The software was calibrated using this scale, and muscovite grains were measured for thickness. The orientation was carefully examined to ensure that a true thickness determination was made. Plates that presented an edge view at or near perpendicular angles were measured, as in Figure 19.

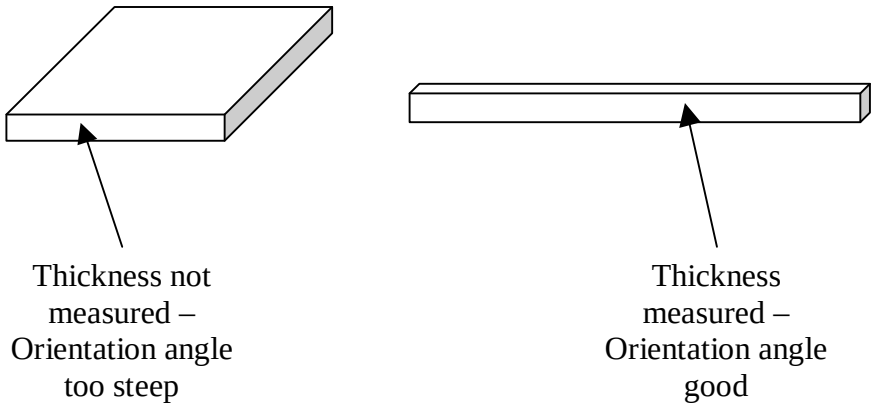

Figure 19. Orientation angle in thickness measurement

4.2.2 Feed Sample <100 Mesh and Baseline Grind Test

There were between ten and fifteen images taken for each composite sample. Table 10 is an index of the all the SEM photographs used for measurements. For the feed sample analysis, fifteen images were captured using the Quartz 5.5 software.

Table 10. SEM photograph index

Sample	Microwave Irradiation	Photograph Number
Feed Sample <100 mesh	No	1a, 1b, 1c, …
Grind Test Baseline	No	2a, 2b, 2c, …
HCl Leach 1 Hour	Yes	7a, 7b, 7c, …
HCl Leach 2 Hours	Yes	8a, 8b, 8c, …
HCl Leach 4 Hours	Yes	9a, 9b, 9c, …
HCl Leach 8 Hours	Yes	3a, 3b, 3c, …
HCl Leach 8 Hours	No	4a, 4b, 4c, …
$LiNO_3$ Leach 1 Hour	Yes	10a, 10b, 10c, …
$LiNO_3$ Leach 2 Hours	Yes	11a, 11b
$LiNO_3$ Leach 4 Hours	Yes	12a, 12b, 12c, …
$LiNO_3$ Leach 8 Hours	Yes	5a, 5b, 5c, …
$LiNO_3$ Leach 8 Hours	No	6a, 6b, 6c, …

There were 74 measurements taken from these images, with an average thickness calculated at 5.9 μm. Figure 20 shows image 1e. Note the measurement of the mica plate in the centre of the image. The plate edges were identified visually by differences in greyscale, and the arrow markers were placed where the border of the mica edges and plane meet.

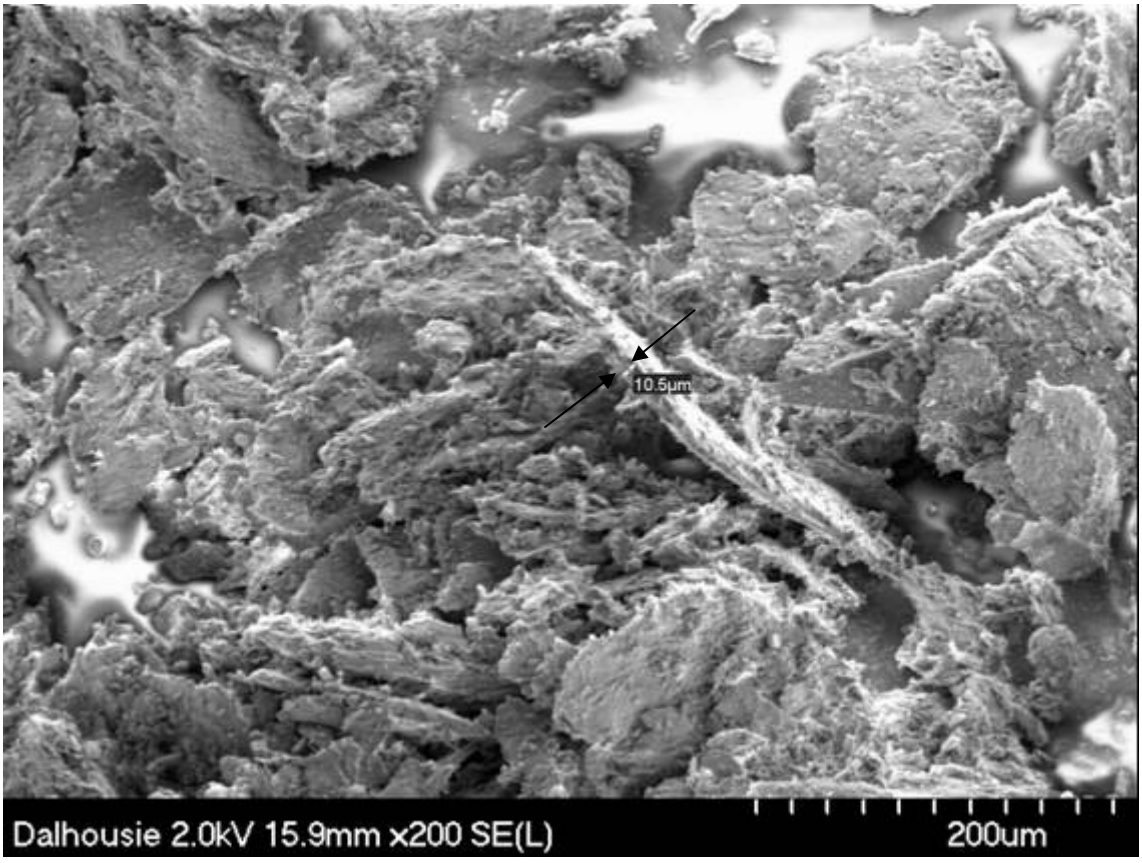

Figure 20. Feed sample <100 mesh, image 1-e

Thirteen images were taken of the mica from the base line grind test. From these images, forty-six thickness measurements were made. The average thickness was calculated to be 5.8 μm. Figure 21 shows an SEM image of mica from the baseline grind test.

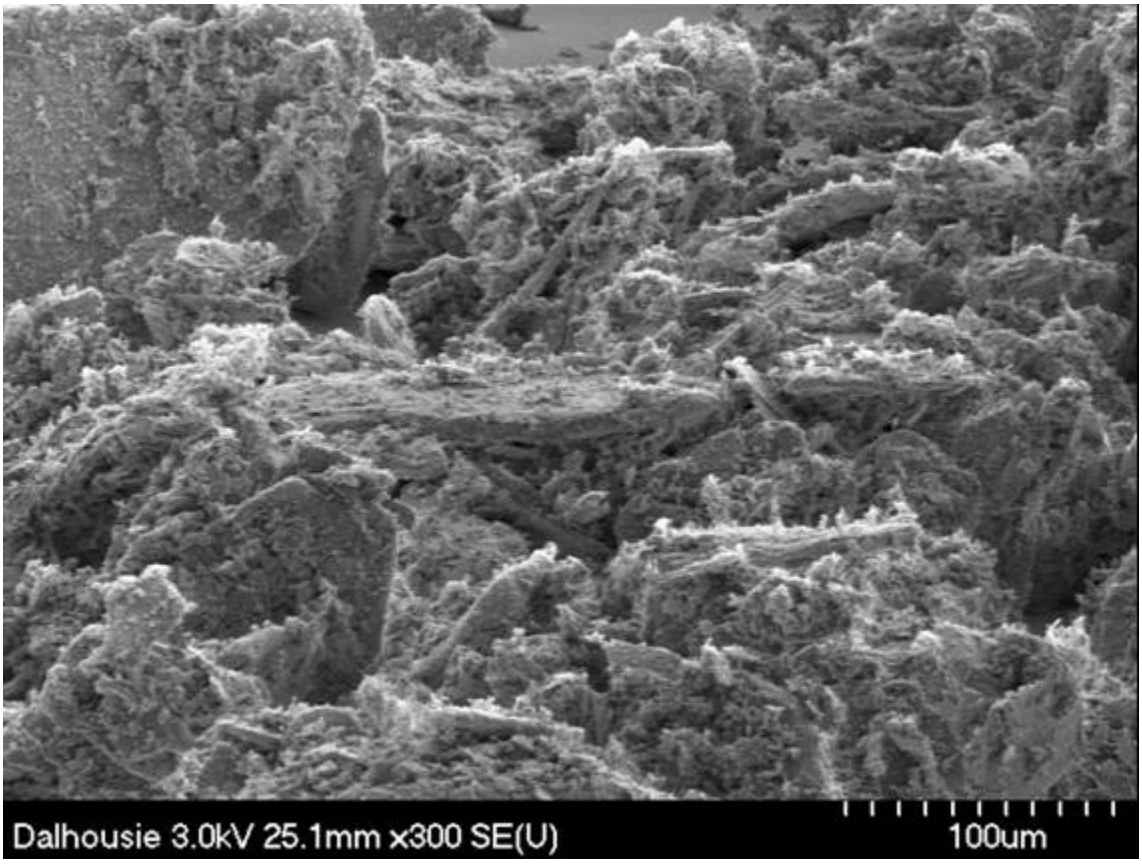

Figure 21. Baseline grind test, image 2-f

4.2.3 Hydrochloric Acid Leach

4.2.3.1 HCl One Hour Leach

Figure 22 shows an image of mica plates after a one hour HCl leach. For the HCl one-hour leach, eleven SEM images were captured. A total of 84 measurements were made, with an average thickness calculated to be 4.2 μm.

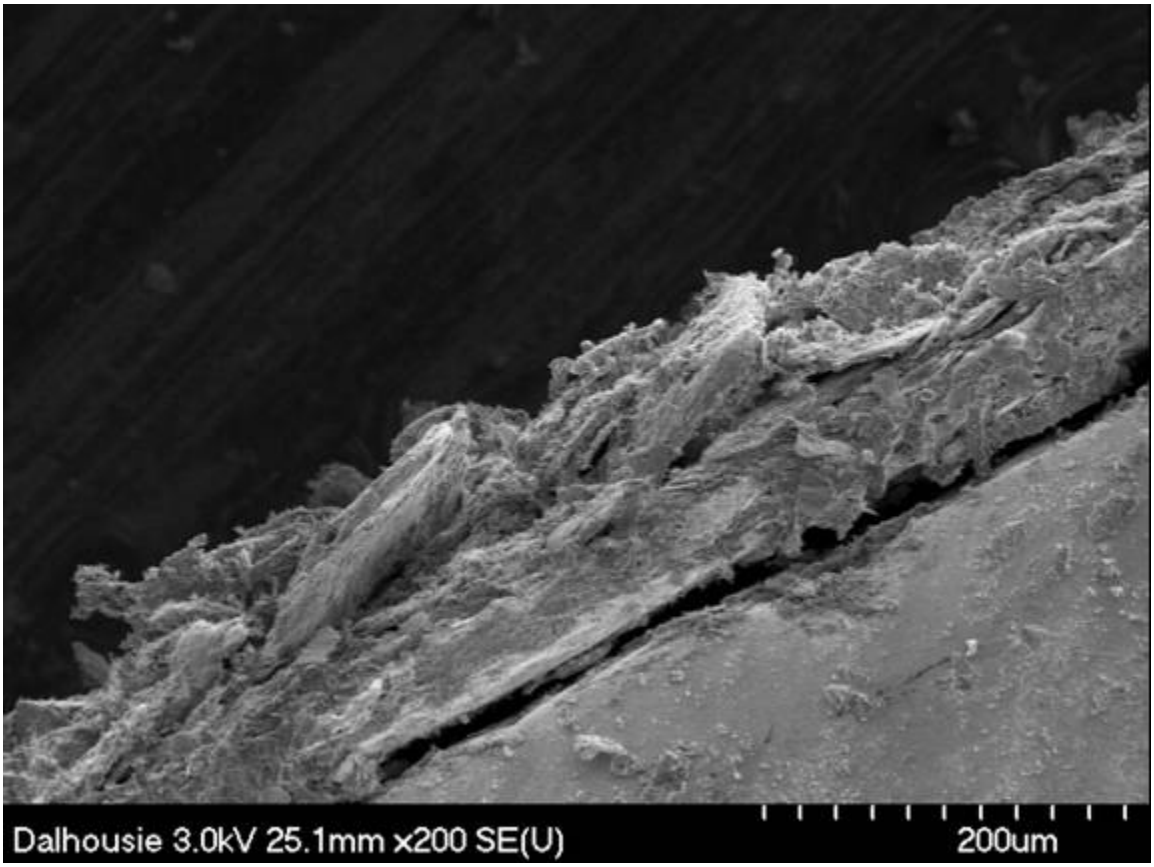

Figure 22. HCl leach one hour, image 7-m

For the HCl leach experiment, average particle thickness versus time can be found in Table 11. Average plate thickness was calculated using all measurements taken from the SEM images. A summary of all thickness measurements for the HCl leach tests is found in Table 22 in Appendix A.

Table 11. Average particle thickness HCl leach

Sample	Leach Time (hours)	Average Thickness (microns)	Average Thickness Standard Deviation
HCl + Microwave	1	4.2	1.9
HCl + Microwave	2	4.5	1.8
HCl + Microwave	4	3.6	1.6
HCl + Microwave	8	4.0	2.5
HCl No Microwave	8	5.0	1.9

4.2.4 Lithium Nitrate Leach

Figure 23 shows an image of mica after 8 hours leach in lithium nitrate. In this test, twelve images were taken and 97 measurements were made. The average thickness was determined to be 3.5 μm.

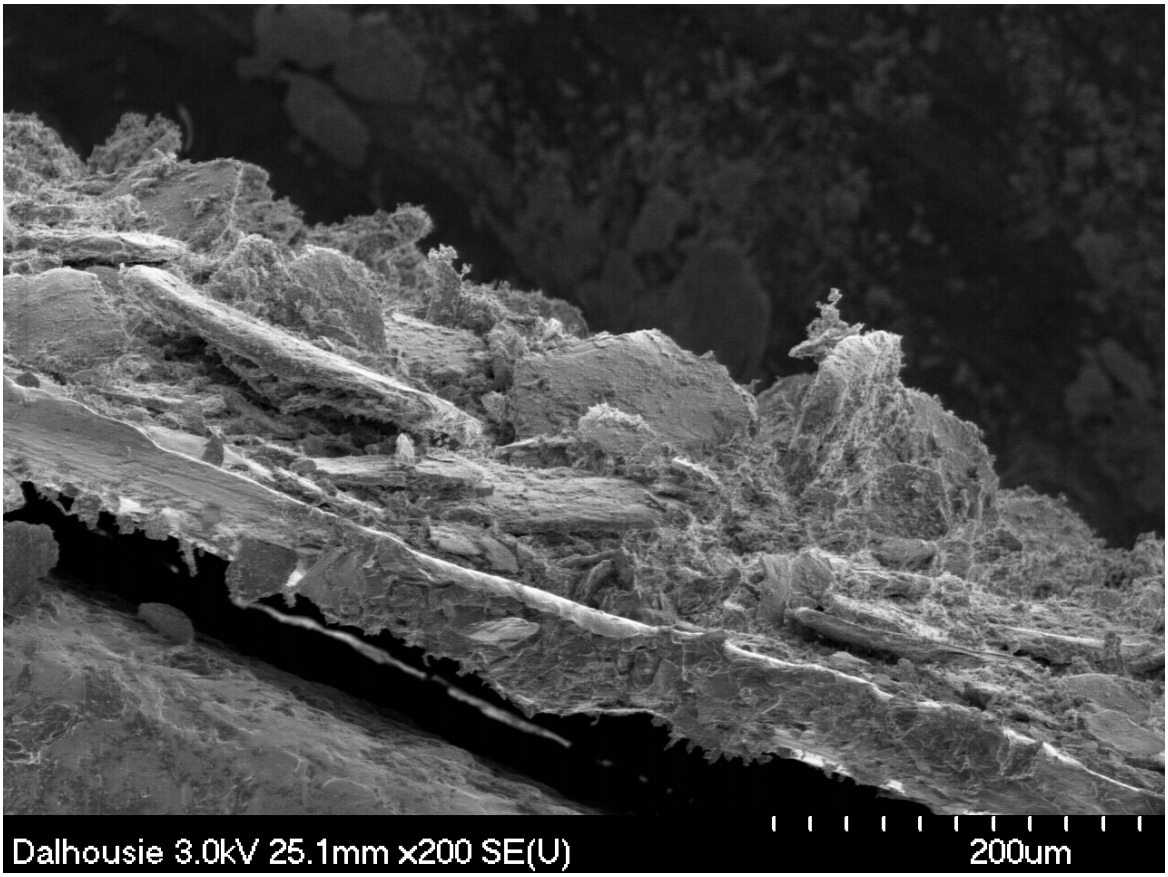

Figure 23. Lithium nitrate leach 8 hours, image 5-m

The average thickness for all of the lithium nitrate leach tests can be seen in Table 12. Table 24, Table 25, and Table 26 summarise the lithium nitrate leach thickness measurements and are found in Appendix A.

Table 12. Average particle thickness lithium nitrate leach tests

Sample	Leach Time (hours)	Average Thickness (microns)	Average Thickness Standard Deviation
$LiNO_3$ + Microwave	1	5.0	2.5
$LiNO_3$ + Microwave	2	4.7	1.5
$LiNO_3$ + Microwave	4	4.1	1.9
$LiNO_3$ + Microwave	8	3.5	1.3
$LiNO_3$ + No Microwave	8	4.6	2.0

4.3 Aspect Ratio Calculation

4.3.1 Feed Sample and Baseline Grind Test

The aspect ratios of the “Feed Sample <100 mesh” and the “GT Baseline” test were calculated using the data from the Malvern particle size distribution and the SEM image analysis. The ratio was calculated by dividing the Malvern average particle size (d_{50}) by the average thickness measured in the SEM image analysis. The resulting aspect ratio was not to be used as an absolute value, but as a relative value for comparison purposes.

The results of the aspect ratio for the "Feed Sample <100 mesh" and the "GT Baseline" test are shown in Table 13.

Table 13. Calculated aspect ratio of feed sample <100 mesh and GT baseline

Sample	Leach Time (hours)	Average Thickness (microns)	Average Thickness Standard Deviation	Malvern Average Particle Size (d_{50})	Aspect Ratio
Feed Sample <100 mesh	0	5.9	2.7	71.9	12.1
GT Baseline	0	5.8	2.3	43.0	7.4

4.3.2 Hydrochloric Acid Leach

The aspect ratio results for 1, 2, 4 and 8-hour leaches are shown in Table 14. Figure 24 shows a graph of average particle thickness vs. time for the HCl leach tests.

Table 14. Calculated aspect ratio of HCl leach tests

Sample	Leach Time (hours)	Average Thickness (microns)	Malvern Average Particle Size (d_{50})	Aspect Ratio
HCl + Microwave	1	4.2	42.5	10.1
HCl + Microwave	2	4.5	42.9	9.5
HCl + Microwave	4	3.6	41.5	11.7
HCl + Microwave	8	4.0	47.1	11.7
HCl No Microwave	8	5.0	49.9	9.9

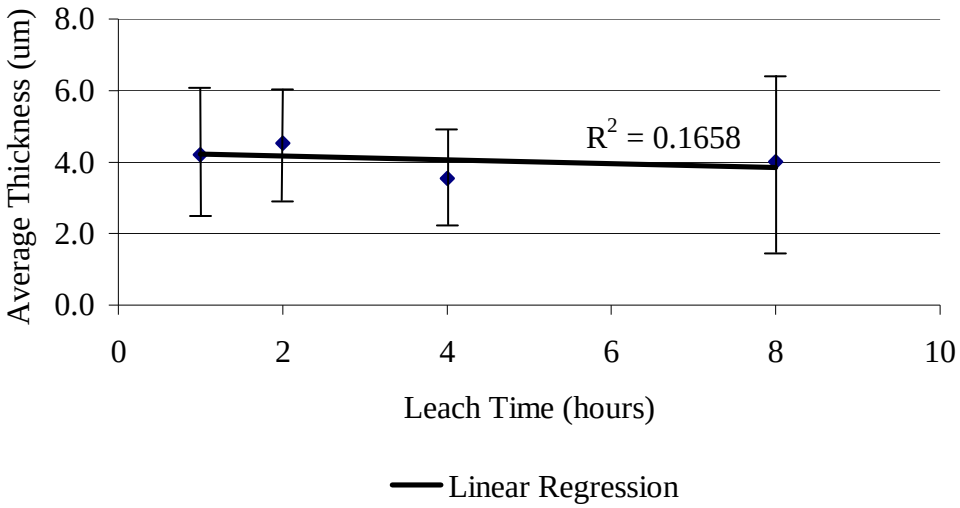

Figure 24. HCl leach particle thickness (µm) vs. time (hrs). Error bars represent one standard deviation.

A graph showing aspect ratio vs. time is shown in Figure 25.

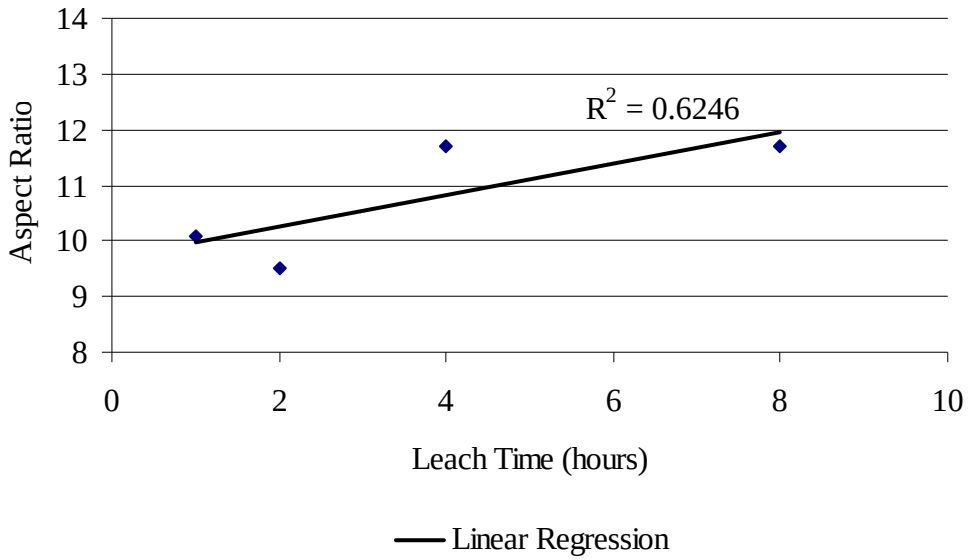

Figure 25. HCl leach mica aspect ratio

4.3.3 Lithium Nitrate Leach

The aspect ratio results for 1, 2, 4 and 8-hour leaches are shown in Table 15.

Table 15. Calculated aspect ratio of $LiNO_3$ leach tests

Sample	Leach Time (hours)	Average Thickness (microns)	Malvern Average Particle Size (d_{50})	Aspect Ratio
$LiNO_3$ + Microwave	1	5.1	45.4	8.9
$LiNO_3$ + Microwave	2	4.7	45.1	9.6
$LiNO_3$ + Microwave	4	4.1	46.8	11.4
$LiNO_3$ + Microwave	8	3.5	46.1	13.1
$LiNO_3$ + No Microwave	8	4.6	48.3	10.6

A graph of particle thickness vs. time for the lithium nitrate leach tests is shown in Figure 26.

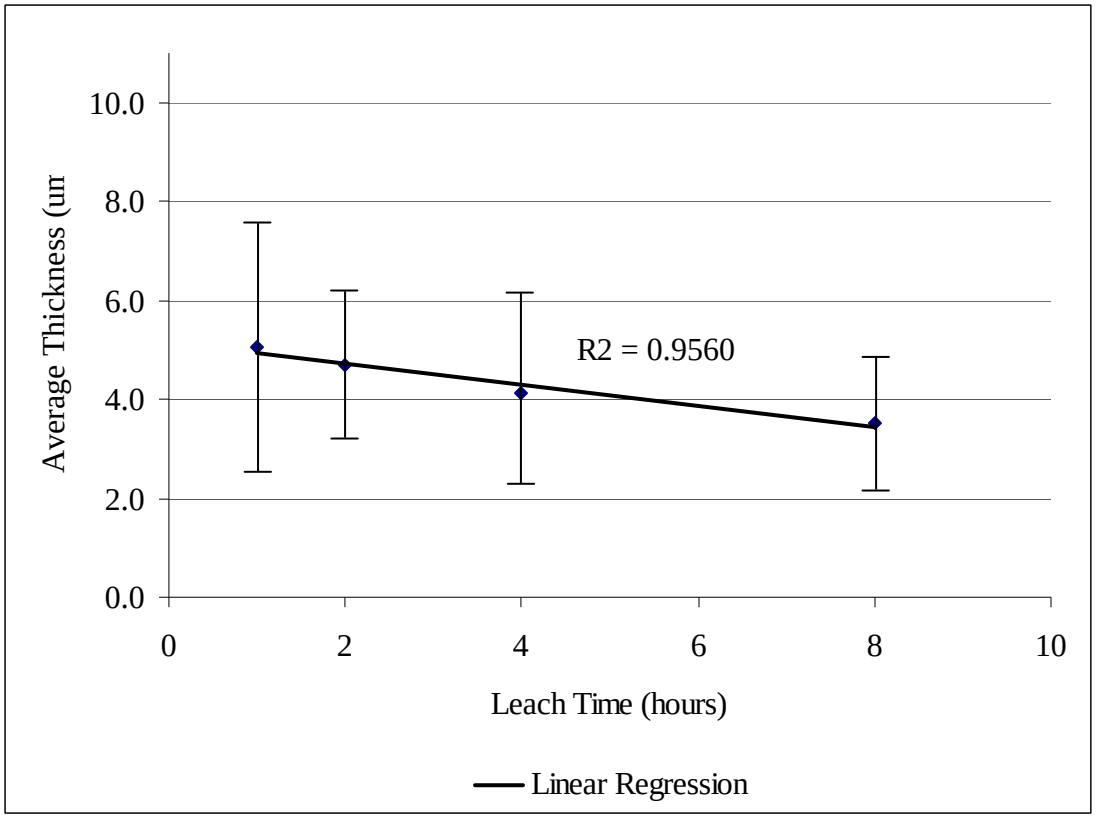

Figure 26. Lithium nitrate leach particle thickness (µm) vs. time (hrs). Error bars represent one standard deviation.

Mica aspect ratio vs. time is shown in Figure 27 for the lithium nitrate leach.

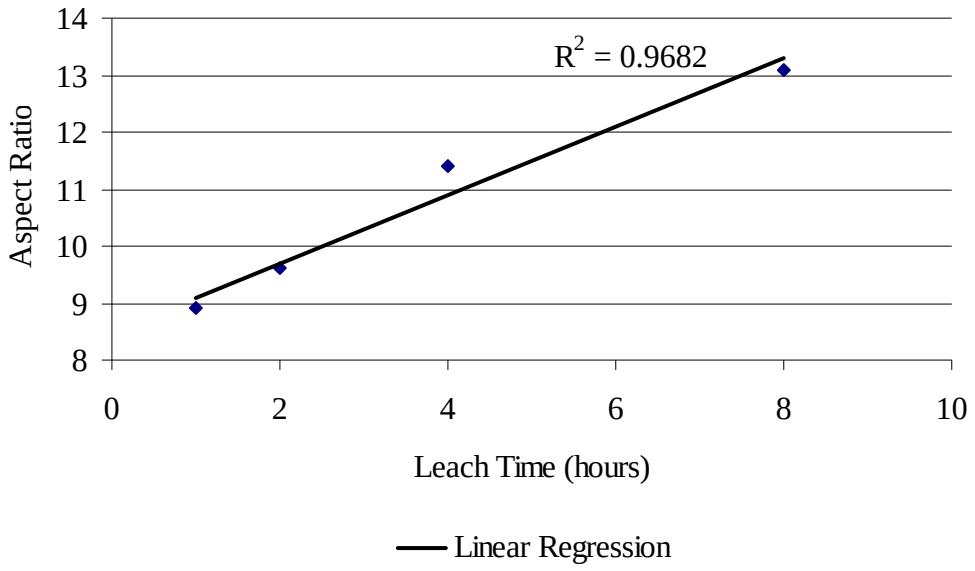

Figure 27. Lithium nitrate leach mica aspect ratio (d_{50})

5 Discussion

5.1 Particle Size Distribution

5.1.1 Feed Sample and Baseline Grind Test

The feed sample initially had a d_{50} of 71.9 microns, while the ground sample had a d_{50} of 43.0 microns. The grind test indicated that the coffee grinder reduced the average size distribution of the mica feed sample. It is assumed that the size reduction is occurring along the x and y axis of the mica plates. The laser diffraction method does not measure the thickness of the plates, but measures the plate width.

5.1.2 Hydrochloric Acid Leach

The results of the size distribution analysis are shown in Figure 15, page 44. The results indicate that there is little difference between the 1 to 8 hour leach tests. The HCl leach was not expected to have an effect on the x or y dimensions of the mica plates, after grinding. However, the 8-hour leach size distribution indicated a slightly coarser grind. This could be explained by variance in the Malvern particle size analysis, or possibly due to the dissolution of the ultra fine, sub-micron particles in the 8-hour leach. If some of the ultra fine particles were dissolved in hydrochloric acid, the particle size distribution curve would be skewed to the right, as it is here. As such, the size analysis did not reveal any significant difference in how the particles responded to the acid treatment over the 8-hour test.

For the microwave control test, there was little difference in the particle size distribution between the HCl 8-hour leach test with microwave irradiation and the HCl 8-hour leach with no microwave irradiation. The microwave irradiation did not seem to have any

effect on the particle size distribution. Figure 16 shows the d_{50} for the HCl 8-hour leach test was 47.1 μm, while the d_{50} for the HCl 8-hour control test was 49.9 μm.

5.1.3 Lithium Nitrate Leach

The results of the lithium nitrate leach revealed that there was almost no difference in particle size distribution among the tests. The longer leach residence times did not have an effect on how the mica responded to the grinding process, with respect to particle size distribution. A graph of the various particle size distributions can be seen in Figure 17, page 46.

The results of the microwave control test, Figure 18, page 47, revealed that there was virtually no difference in the particle size distribution of the microwave irradiated and non-irradiated samples. The lithium nitrate solution did not seem to change the x or y dimensions of the mica plates after grinding.

5.2 Mica Thickness Measurements

5.2.1 Feed Sample and Baseline Grind Test

The average particle thickness of the feed sample was determined to be 5.9 μm, while the baseline grind test produced particles with an average thickness of 5.8 μm. From this result, it appears that grinding the untreated non-microwave irradiated feed sample will not significantly change the particle thickness. This has important implications for the leaching experiments. That is, any changes to particle thickness in the chemical treatment tests can be attributed to other factors other than the coffee grinder.

The coffee grinder appears to function like a hammer mill (section 2.5.4) and mica size reduction occurs primarily on the x and y axis.

5.2.2 Hydrochloric Acid Leach

For the HCl leach test, the thickness of the mica plates did not seem to change over time. Variations in average particle thickness are most likely due to measurement error. The linear regression equation in Figure 24 indicated a poor fit for the trend line.

However, all of the HCl leach tests resulted in mica plates with a thickness less than the GT Baseline test. A possible explanation for this effect may be that the HCl treatment allowed hydroxyl ions to penetrate into already existing cracks or "frayed edges" of the mica plates. These frayed edges may have been in place before or after the initial sample preparation of the –100 mesh feed material.

Experiments done by Kalinowski and Schweda (1996) on artificial weathering of mica suggests that low pH will cause exfoliation of the mica plates. It is not clear in this experiment that exfoliation of more "intact" mica plates has occurred. The exfoliation rate may occur at a level that is not measurable within the parameters of this experiment.

5.2.3 Lithium Nitrate Leach

The results of the lithium nitrate leach experiment indicated that the mica thickness decreased over time. The initial plate thickness was 5.9 microns and decreased to 3.5 microns in the eight-hour leach. The linear regression for the trend line in Figure 26 indicated good correlation.

Leaching alone with no microwave treatment seemed to have a small effect on the plate thickness. This delamination effect may have occurred by a similar mechanism as explained earlier in the Caseri process. The difference in average mica thickness between the 8-hour leach with microwave irradiation and without irradiation is significant. The average plate thickness for 8-hour microwave irradiated mica was 3.5 microns, and for the non microwave irradiated mica the average was 4.6 microns. This difference indicates that the microwave irradiation is having some effect on the delamination of the mica.

While there appears to be delamination occurring, the average mica plate thickness did not approach the values reported by Caseri. The most probable explanation for this is that the lithium nitrate concentration in this experiment was lower than what Caseri used. In addition, the leach time in this experiment was shorter and the leach temperature was lower.

It is not clear from the graph in Figure 26 if the rate of delamination of mica indicates a linear or an exponential function. The 8-hour experiment may be too brief in order to determine this function.

5.3 Aspect Ratio

5.3.1 Feed Sample and Baseline Grind Test

In Table 13, page 56, the average thickness of the mica plates in the feed sample was 5.9 microns. The average particle size was 71.9 microns, producing an aspect ratio of 12.1 diameter to thickness. For the GT baseline test, the average mica thickness was determined to be 5.8 microns. The average particle size was 43.0 microns. The GT baseline aspect ratio was found to be 7.4.

From the data in Table 13 it can be seen that the aspect ratio is not preserved in the grinding of untreated muscovite mica. While the mica thickness was not affected by the grinding action, the average particle size was reduced. This in turn reduced the aspect ratio of the mica plates from 12.1 to 7.4.

5.3.2 Hydrochloric Acid Leach

There was no noticeable change in aspect radio for the HCl leach and grind test during the experimental time period. Average particle thickness and width remained fairly constant following the one to eight hour leaches. However, all of the leaching tests with HCl produced mica with a slight but significantly higher aspect ratio after grinding than with grinding alone. In Table 13, the aspect ratio of the grind test baseline was 7.4 microns. Table 14, page 56, shows that the HCl leached mica had aspect ratios ranging from 9.5 to 11.7. The slightly higher aspect ratios are the result of an overall decrease in average plate thickness, and not from any changes in the average plate width.

5.3.3 Lithium Nitrate Leach

Lithium nitrate treatment combined with microwave irradiation appears to increase the aspect ratio of the mica plates. The average plate thickness decreased over time during the experiments, while grinding produced plates with a relatively consistent diameter. The eight-hour test with no microwave irradiation also had a slight increase in aspect ratio compared to the baseline grind test. As mentioned in section 5.2.3, the decrease in average plate thickness may have occurred by a mechanism similar to the delaminating process described by Caseri (1992).

6 Conclusion

Hydrochloric acid did not have a significant effect on the thickness of mica plates after microwave irradiation. There was no apparent trend with respect to the plate thickness and leach time. The mica plates averaged 3.6 microns to 4.5 microns in the leach tests. The calculated aspect ratios were found to be between 9.5 and 11.7.

There was, however, a reduction of plate thickness for all of the HCl leach tests in comparison to the GT baseline test. The mechanism for this reduction is not entirely clear, but it may be explained by pre-existing partial openings or frayed edges. Initial exfoliation that occurred may be a result of these pre-existing frayed edges, and any further exfoliation of the mica plates may occur at a rate not measurable in this experiment.

Chemical treatment with lithium nitrate and microwave irradiation produced higher aspect ratios in muscovite mica than with chemical treatment alone. Mica plate thickness decreased from 5.1 microns to 3.5 microns. The calculated aspect ratio of the lithium nitrate treated microwave irradiated mica increased over time from 8.9 to 13.1.

In the lithium nitrate experiment, the aspect ratio of non-microwave irradiated mica increased in comparison to the GT baseline test. The aspect ratio of the GT baseline mica was 7.4. The aspect ratio of the lithium nitrate leached, non-microwave irradiated mica was 10.6. This effect is supported by research conducted by Caseri (1992). Casari described a possible explanation for this effect in that the lithium nitrate hydrated the potassium layers. Once hydrated, the layers are more easily delaminated, possibly by shear forces while mixing or grinding.

7 Recommendations

The lithium nitrate-microwave irradiation appears to have increased the aspect ration of mica plates. Some variables, such as lithium nitrate concentration, leach times, and microwave irradiation duration could be examined. More specifically, microwave energy power may have a significant influence on the outcome of this experiment. It is conceivable that lithium nitrate treated mica may produce higher aspect ratios if the mica were irradiated with a focused beam of high power microwave energy.

For this thesis, a commercial 1 kilowatt microwave oven was used. During the irradiation phase, some of the water in the "frayed edges" of the weathered mica may have heated and evaporated too slowly. The desired microwave effect is a rapid, almost violent evaporation of the hydrated edges. A more rapid evaporation may provide better success in delaminating the layers.

The performance of the chemically treated mica plates with respect to plastic filler properties should be evaluated. Test work should be performed to examine rigidity and dimensional stability of the plastic matrix produced by lithium nitrate leaching-microwave irradiation.

References

Al-Harahsheh, M., Kingman, S.W., Microwave-assisted leaching-a review, Hydrometallurgy, 2004, Vol. 73, pp. 189-203

Azco Mining Inc., Information About Mica [Online] Available: http://azco.com/mica/micainfo.php [Nov 4, 2008]

Bardet, J. J., US Patent 2549880, April 24, 1951. Methods for Treating Mica and Composition

Black, D., personal communication, Truro, Nova Scotia, Canada

Bowen, P., Sheng, J., Jongen, N., Particle size distribution measurement of anisotropic-particles cylinders and platelets-practical examples, Powder Technology, Volume 128, 2002, pages 256-261

Bradshaw, S.M., Applications of microwave heating in mineral processing, South African Journal of Science 95, September 1999, p. 394-396

Brady, N., The Nature and Properties of Soils, 8th edition, pp 282-283, Macmillan Publishing Co., Inc., New York 1974

Caseri, W. R., Shelden, R. A., Suter, U. W. Preparation of Muscovite With Ultrahigh Specific Surface Area by Chemical Cleavage, Colloid & Polymer Science, 1992, 270:392-398.

Chaplin, M. Electronic Sources: Water and Microwaves [online]. Available: http://www.lsbu.ac.uk/water/microwave.html [2008, 25 June]

Chen, T.T., Dutrizac, J.E., Haque, K.E., Wyslouzil, W., Kashyap, S. The relative transparency of minerals to microwave radiation. Canadian Metallurgy Quarterly, 1984, Vol. 23, No. 3, 349-351.

Fanning and Keramidas, pp 195-251, Chapter 7, Micas, in Minerals in Soil Environments, Soil Science Society of America, Madison Wisconsin, USA, 1977

Gaines, R.V., Skinner, H., Foord, E, Mason, B., Rosenzweig, A., King, V., Dowty, E., Dana's New Mineralogy 8th Edition, 1997, pp 1444-1449. John Wiley & Sons, Inc., 605 Third Avenue, New York, NY 10158-0012

Galema, S.A., 1997. Microwave chemistry. Chemical Society Reviews 26, 233-238.
Harben, P. 1999. Industrial Minerals HandyBook. 3rd ed. London: Metal Bulletin PLC

Hedrick, J., Mica, U.S. GEOLOGICAL SURVEY MINERALS YEARBOOK-2002

Hendrik, H., Castelijns, H., and Suter, U., Structure and Phase Transitions of Alkyl Chains on Mica, Department of Materials, Institute of Polymers, ETH, CH-8092 Zürich, Switzerland, 7/4/03

Hohenberger, W. Holzinger, T. Bernhart, W. Processing - Mineral Aspect Ratio, Industrial Minerals, 2002, n. 422, 64-69

Kalinowski, B., Schweda, P., Kinetics of muscovite, phlogopite, and biotite dissolution and alteration at pH 1-4, room temperature, Geochimica et Sjosmochimica Acta, Vol. 60 No. 3, pp367-385, 1996.

Kauffman, S.H., Leidner, J., Woodhams, R.T., Xanthos, M., Powder Technology, Vol 9, pages 125-133, 1974

Kingman, S. W., Vorster, W., Rowson, N. A. The Influence of Mineralogy on the Microwave Assisted Grinding, Minerals Engineering, 2000, Vol. 13. No. 3 pp. 313-327.

Malvern Instruments Particle Sizer Reference Manual, Manual Version 3.0, 22 July 1986, Spring Lane, Malvern, Worcestershire, WR14 1Aq, England

Microtrac Inc., Laser Diffraction - Mie Scattering Theory [online] Available: http://www.microtrac.com/laserdiffraction.cfm

Orumwense, A.O., Negeri, T., Impact of microwave irradiation on the processing of a sulfide ore, Minerals & Metallurgical Processing, Feb 2004, Vol 21 No. 1 pp 44-51

Sims, C., Industrial Minerals, January 1997, p.29

Skillen, A., Industrial Minerals, Issue 25, November 1992, Metal Bulletin Ltd. London

Taggart, A. F., Handbook of Minerals Dressing-Ores and Industrial Minerals, Section 6-06, New York John Wiley & Sons, Inc, London: Champan & Hall, 1950

Walkiewicz, J. W., Clark, K. E., McGill, S. L., Microwave-Assisted Grinding, IEEE Transactions on Industry Applications, Vol. 27, No. 2, March/April 1991 pp 239-243

Walkiewicz, J. W., Kazonich, G., McGill, S. L., 1988. Microwave heating characteristics of selected minerals and compounds. Mineral and Metallurgical Processing 5 (1), 39-42

Appendices

Appendix A

Size Analysis Raw Data

The following Table 16, Table 17, and Table 18, are a summary of the size distribution analysis results for the feed sample, GT composite sample, HCl leach test, and lithium nitrate leach test. The size distribution results from the Malvern particle size analysis follows in Table 19 and Table 20.

Table 16. Particle size data for feed <100 mesh and feed sample GT composite.

	Feed <100 Mesh	Feed Sample GT comp
D (v, 0.5)	71.9	43.0
D (v, 0.9)	179.0	124.7
D (v, 0.1)	7.8	6.2
D (4,3)	80.3	57.4
D (3,2)	24.7	17.3

Table 17. Particle size data for HCl 1, 2, 4, and 8 hour leach.

	HCl Treated 1 hr GT Comp (with micro)	HCl Treated 2 Hrs GT Comp (with micro)	HCl Treated 4 hr GT Comp (with micro)	HCl Treated 8 hr GT Comp (with micro)	HCl Treated 8 hr GT comp (no micro)
D (v, 0.5)	42.5	42.9	41.5	47.1	49.9
D (v, 0.9)	125.8	126.7	123.0	134.6	141.1
D (v, 0.1)	6.6	6.6	6.6	7.0	7.3
D (4,3)	57.1	57.2	55.4	63.1	66.1
D (3,2)	18.0	14.2	15.9	20.8	20.0

Table 18. Particle size data for $LiNO_3$ 1, 2, 4, and 8 hour leach.

	$LiNO_3$ Treated 1 hr GT Comp (with micro)	$LiNO_3$ Treated 2 Hrs GT Comp (with micro)	$LiNO_3$ Treated 4 hr GT comp (with micro)	$LiNO_3$ Treated 8 hr GT comp (with micro)	$LiNO_3$ Treated 8 hr GT comp (no micro)
D (v, 0.5)	45.4	45.1	46.8	46.1	48.3
D (v, 0.9)	127.6	126.5	130.1	131.3	132.9
D (v, 0.1)	6.3	6.3	6.4	6.4	6.4
D (4,3)	59.3	59.3	61.2	61.4	62.5
D (3,2)	14.1	17.5	14.2	18.1	18.2

Table 19. PSD feed sample, GT test composite, and HCl leach 1-8 hours

	Cumulative % Under						
Particle Size (Microns)	Feed <100 Mesh	Feed Sample Grind Test Comp	HCl Leach 1 hr GT Comp Micro	HCl Leach 2 hr GT Comp Micro	HCl Leach 4 hr GT Comp Micro	HCl Leach 8 hr GT Comp Micro	HCl Leach 8 hr GT Comp No Micro
564.0	100.0	100.0	100.0	100.0	100.0	100.0	100.0
487.0	100.0	100.0	100.0	100.0	100.0	99.9	99.9
420.0	100.0	99.9	99.9	100.0	100.0	99.8	99.8
362.0	100.0	99.8	99.9	99.9	99.9	99.6	99.5
312.0	99.4	99.7	99.8	99.9	99.8	99.4	99.3
270.0	98.3	99.6	99.7	99.8	99.8	99.3	99.2
233.0	96.4	99.6	99.7	99.8	99.8	98.9	98.7
201.0	93.4	99.2	99.3	99.3	99.7	97.7	97.3
173.0	88.8	98.0	97.3	97.8	98.6	95.6	94.9
149.0	82.5	95.3	95.1	94.9	95.9	92.6	91.5
129.0	75.1	91.1	90.8	90.6	91.6	88.7	87.2
111.0	67.3	85.6	85.6	85.3	86.2	83.4	81.6
95.0	60.4	79.4	80.1	79.9	80.7	77.1	75.2
82.7	54.6	73.4	74.5	74.3	75.3	70.6	68.7
71.4	49.8	68.3	69.2	69.0	70.3	64.9	62.9
61.6	45.1	63.2	63.8	63.4	64.9	59.5	57.5
53.1	40.2	57.7	58.3	57.7	58.9	54.3	52.2
45.8	35.6	52.3	52.7	52.3	53.3	49.0	47.0
39.5	31.7	47.0	47.4	47.2	48.3	43.9	42.0
34.1	28.7	42.3	42.5	42.4	43.5	39.7	37.9
29.4	26.3	38.5	38.5	38.5	39.4	36.3	34.5
25.4	24.2	35.7	35.4	35.6	36.4	33.3	31.6
21.9	21.8	32.6	32.1	32.3	32.9	30.0	28.4
18.9	19.3	29.0	28.3	28.4	28.9	26.5	25.0
16.3	17.0	25.5	24.7	24.6	25.1	23.0	21.7
14.1	15.2	22.5	21.7	21.7	22.1	20.1	18.9
12.1	13.8	20.2	19.2	19.3	19.6	17.7	16.7
10.5	12.6	18.3	17.1	17.2	17.4	15.7	14.8
9.0	11.3	16.3	14.9	15.0	15.0	13.7	12.9
7.8	10.0	14.4	13.0	13.1	13.0	11.7	11.0
6.7	8.0	11.7	10.4	10.5	10.4	9.2	8.7
5.8	5.7	8.3	7.3	7.3	7.2	6.4	6.0

Table 20. Particle size distribution $LiNO_3$ leach 1, 2, 4, and 8 hours.

Particle Size (Microns)	Cumulative % Under				
	$LiNO_3$ Leach 1 hr GT Comp Micro	$LiNO_3$ Leach 2 hr GT Comp Micro	$LiNO_3$ Leach 4 hr GT Comp Micro	$LiNO_3$ Leach 8 hr GT Comp Micro	$LiNO_3$ Leach 8 hr GT Comp No Micro
564.0	100.0	100.0	100.0	100.0	100.0
487.0	100.0	100.0	100.0	100.0	100.0
420.0	99.9	99.9	99.8	99.9	99.9
362.0	99.8	99.8	99.7	99.7	99.8
312.0	99.8	99.7	99.5	99.6	99.6
270.0	99.7	99.7	99.3	99.5	99.5
233.0	99.5	99.4	99.1	99.3	99.3
201.0	98.8	98.7	98.3	98.5	98.3
173.0	97.2	97.0	96.6	96.8	96.4
149.0	94.4	94.4	93.8	93.7	93.3
129.0	90.3	90.6	89.7	89.4	89.0
111.0	84.9	85.4	84.1	83.6	83.2
95.0	78.8	79.1	77.6	77.0	76.6
82.7	72.4	72.5	71.1	70.6	70.0
71.4	66.6	66.3	65.4	65.4	64.5
61.6	61.0	60.7	60.0	60.4	59.2
53.1	55.6	55.5	54.6	55.1	53.6
45.8	50.3	50.5	49.2	49.8	48.0
39.5	45.4	45.7	44.1	44.6	43.0
34.1	41.1	41.5	39.9	40.0	39.1
29.4	37.8	38.0	36.7	36.3	36.0
25.4	35.1	35.2	34.0	33.6	33.5
21.9	32.0	32.2	31.1	30.7	30.6
18.9	28.4	28.6	27.9	27.3	27.2
16.3	24.8	25.1	24.6	23.9	23.8
14.1	21.9	22.2	21.8	21.2	21.0
12.1	19.8	20.0	19.5	19.1	18.9
10.5	18.0	18.3	17.7	17.3	17.2
9.0	16.2	16.4	15.9	15.4	15.6
7.8	14.3	14.5	14.0	13.7	13.8
6.7	11.5	11.7	11.2	11.1	11.2
5.8	8.1	8.3	7.9	7.9	7.9

SEM Size Analysis Raw Data

The following Table 21,Table 22,Table 23,Table 24,Table 25, and Table 26 are of the raw data measurements taken from the SEM photographs, found in Appendix B, of the feed sample, GT baseline composite sample, HCl leach tests, and lithium nitrate leach tests.

Table 21. Mica thickness measurement (μm), feed sample, GT baseline

<100 Mesh Feed Sample						GT Baseline Test			
1a	6.7	1e	6.4	1r	6.3	2a	6.5	2h	5.7
1a	4.9	1e	4.9	1r	4.7	2a	5.0	2h	5.7
1a	12.4	1e	7.4	1r	4.7	2b	5.1	2h	4.0
1a	4.0	1f	7.8	1r	2.5	2c	5.8	2h	5.1
1a	2.1	1f	7.5	1r	6.0	2c	7.4	2i	7.6
1a	15.1	1f	5.1	1s	7.7	2d	12.3	2i	4.7
1a	5.9	1i	9.5	1s	8.0	2d	7.8	2i	4.7
1b	6.0	1i	4.6	1s	4.9	2d	5.7	2i	3.3
1b	5.4	1i	2.7	1s	2.2	2e	4.8	2i	7.0
1c	3.2	1i	4.0	1s	2.0	2e	4.4	2k	4.0
1c	9.1	1k	5.3	1s	2.9	2f	2.6	2k	3.5
1c	7.3	1k	5.7	1t	5.7	2f	5.7	2k	6.2
1c	4.0	1k	5.8	1t	4.5	2f	2.7	2k	6.3
1c	4.5	1k	6.5	1t	4.6	2f	8.4	2m	4.2
1c	5.0	1m	7.0	1t	3.0	2f	4.3	2m	2.7
1c	3.5	1m	6.0	1t	4.0	2f	4.0	2m	6.1
1d	11.6	1o	5.3	1t	2.9	2f	2.7	2n	11.0
1d	6.5	1o	6.4	1u	4.0	2f	3.0	2n	11.5
1d	13.4	1o	6.3	1u	3.5	2g	6.9	2o	7.8
1d	7.1	1p	3.0	1u	5.3	2g	6.0	2o	8.0
1d	3.2	1p	3.8	1u	9.4	2g	5.0	2o	10.0
1d	3.6	1p	5.8	1u	4.6	2g	5.8		
1e	3.8	1p	8.6	1u	9.3	2g	7.4		
1e	11.7	1r	9.8	1u	7.0	2h	4.0		
1e	5.8	1r	9.2			2h	6.0		

Table 22. Mica thickness measurement (μm), HCl leach 1 and 2 hours.

HCl Leach 1 hr Micro						HCl Leach 2 hr Micro					
7a	6.9	7f	5.0	7k	4.2	8a	3.0	8f	5.3	8k	4.2
7a	3.2	7f	2.5	7k	2.0	8a	4.0	8f	4.3	8k	8.2
7a	3.6	7f	4.5	7k	4.0	8a	7.5	8g	3.5	8k	4.7
7a	4.2	7f	4.7	7k	2.5	8b	5.3	8g	5.9	8k	9.0
7a	4.0	7f	3.0	7k	3.8	8b	3.5	8g	4.9	8k	2.0
7a	3.1	7f	4.0	7m	4.0	8b	4.0	8g	5.0	8k	4.7
7b	3.2	7f	3.9	7m	5.3	8b	3.5	8g	2.5	8k	4.0
7b	3.0	7f	11.1	7m	3.2	8c	2.5	8g	3.0	8k	4.9
7b	3.3	7f	1.6	7m	3.9	8c	4.6	8g	2.7	8k	5.4
7b	5.3	7g	6.8	7m	3.2	8c	5.8	8g	6.5	8k	6.5
7c	1.6	7g	2.5	7m	3.8	8c	4.5	8g	3.1	8k	6.5
7c	5.6	7g	2.5	7m	4.6	8c	5.3	8g	3.1	8m	5.0
7c	3.1	7g	4.1	7m	2.2	8c	3.6	8h	4.5	8m	4.6
7c	3.0	7g	3.0	7m	9.2	8c	4.3	8h	8.8	8m	5.2
7c	3.5	7g	8.7	7m	4.4	8c	1.4	8h	3.6	8m	6.6
7d	3.1	7g	11.1	7m	3.3	8c	6.5	8h	5.5	8m	3.6
7d	2.2	7h	6.9			8c	4.5	8h	7.5	8m	4.7
7d	2.0	7h	7.4			8d	2.7	8h	8.8	8m	8.2
7d	4.3	7h	7.4			8d	2.2	8h	4.0	8m	3.6
7d	3.8	7h	4.4			8d	1.4	8h	4.0	8m	3.6
7d	6.4	7h	4.7			8d	8.5	8h	3.0	8m	6.5
7d	3.6	7h	5.5			8e	3.9	8h	2.9	8m	5.2
7d	3.6	7i	6.7			8e	1.6	8i	8.7	8m	3.5
7d	3.0	7i	3.6			8e	4.3	8i	4.0	8m	2.1
7d	2.7	7i	3.1			8e	3.6	8i	4.0		
7d	3.0	7i	4.3			8e	5.6	8i	2.7		
7d	2.0	7i	5.0			8e	3.2	8i	3.5		
7e	2.7	7i	4.7			8f	2.7	8i	4.2		
7e	6.0	7i	2.8			8f	2.5	8i	6.7		
7e	2.8	7i	2.7			8f	6.3	8i	3.5		
7e	7.1	7i	4.7			8f	2.5	8i	2.9		
7e	5.3	7k	3.2			8f	5.8	8i	5.0		
7e	2.0	7k	2.2			8f	3.3	8i	3.1		
7e	3.1	7k	5.2			8f	4.7	8k	4.7		

Table 23. Mica thickness measurement (μm), HCl leach 4 and 8 hours.

HCl Leach 4 hr Micro								HCl Leach 8 hr Micro				HCl Leach 8 hr No Micro			
9a	4.0	9e	3.0	9g	3.3	9m	2.5	3a	6.1	3h	7.8	4a	4.0	4g	1.8
9b	2.1	9e	5.8	9g	3.5	9n	3.9	3a	1.8	3h	4.5	4a	3.5	4g	3.1
9b	1.6	9e	3.3	9g	2.7	9n	2.5	3b	4.5	3i	4.5	4b	6.8	4g	3.2
9b	2.5	9e	4.7	9g	1.8	9n	2.0	3c	2.9	3i	3.5	4b	5.5	4g	6.0
9b	3.2	9e	3.5	9g	4.1	9n	6.5	3c	2.9	3i	4.9	4b	5.1	4g	7.6
9b	2.2	9e	2.2	9g	2.7	9n	2.5	3c	2.8	3i	3.5	4b	4.5	4h	3.6
9b	3.3	9e	2.0	9i	3.1	9n	3.5	3c	2.0	3i	3.3	4b	5.1	4h	5.3
9b	4.7	9e	6.6	9i	4.7	9n	2.0	3c	4.5	3m	3.5	4c	6.5	4k	5.5
9b	3.6	9f	3.1	9i	3.6	9n	3.0	3c	2.9	3m	5.7	4c	5.0	4k	6.1
9c	3.3	9f	3.6	9i	1.0	9n	5.0	3c	3.0	3m	7.6	4c	3.9	4k	7.4
9c	4.6	9f	4.5	9i	3.3	9n	1.0	3d	2.9	3m	3.6	4c	3.1	4k	6.1
9c	3.6	9f	3.5	9i	1.5	9n	1.1	3d	3.5	3m	6.9	4c	3.5	4k	5.2
9c	2.2	9f	2.0	9i	3.1	9n	2.0	3d	1.6	3o	11.3	4c	4.6	4m	6.5
9c	3.5	9f	3.6	9i	6.0	9n	5.5	3d	3.3	3o	8.1	4d	3.6	4m	15.4
9c	9.2	9f	2.5	9k	4.0	9o	6.0	3d	7.4	3o	5.1	4d	5.7		
9c	9.6	9f	6.0	9k	3.1	9o	6.0	3d	1.5	3o	2.5	4d	3.6		
9c	4.0	9h	2.5	9k	4.9	9o	3.1	3d	5.1	3o	2.8	4d	4.4		
9c	1.6	9h	3.0	9k	4.4	9o	1.4	3d	1.1	3o	6.1	4d	1.5		
9c	2.7	9h	2.0	9k	4.2	9o	5.0	3d	3.0	3p	4.0	4e	2.5		
9d	2.5	9h	6.5	9k	2.5	9o	3.3	3d	3.0	3p	3.3	4e	2.5		
9d	3.6	9h	3.0	9k	4.0	9o	7.5	3d	2.5	3p	2.7	4e	4.3		
9d	4.6	9h	7.7	9k	4.4	9o	1.5	3d	2.7	3p	3.0	4e	11.4		
9d	4.0	9h	3.1	9k	1.8			3d	4.1	3p	1.5	4e	4.0		
9d	2.9	9h	2.5	9k	2.8			3e	3.1	3p	5.0	4e	4.1		
9d	1.6	9h	4.0	9k	2.0			3e	2.5			4e	4.7		
9d	4.5	9h	2.5	9m	3.0			3e	4.3			4e	4.6		
9d	6.0	9h	2.0	9m	5.4			3e	1.8			4e	9.8		
9d	4.5	9g	3.5	9m	1.6			3e	5.8			4f	5.8		
9d	4.5	9g	3.0	9m	2.8			3e	4.7			4f	7.5		
9d	3.5	9g	1.5	9m	4.3			3e	6.0			4f	2.5		
9d	3.1	9g	2.0	9m	3.9			3e	2.5			4f	1.6		
9e	3.5	9g	3.0	9m	1.6			3e	2.5			4f	4.6		
9e	2.5	9g	4.0	9m	4.0			3e	4.6			4f	5.7		
9e	7.3	9g	4.5	9m	4.0			3h	4.7			4g	3.6		

Table 24. Mica thickness measurement (μm), $LiNO_3$ leach 1 and 2 hours.

$LiNO_3$ Leach 1 hr Micro						$LiNO_3$ Leach 2 hr Micro	
10a	8.8	10d	5.5	10i	2.7	11a	6.0
10a	5.0	10d	3.0	10i	3.3	11a	4.2
10a	3.5	10e	5.3	10i	6.0	11a	3.5
10a	10.7	10e	5.1	10i	5.0	11a	6.0
10a	3.0	10e	9.3	10i	2.9	11b	3.5
10a	6.0	10e	4.6	10i	3.1	11b	7.7
10a	2.0	10e	3.0	10k	8.9	11b	2.7
10a	3.3	10e	5.7	10k	3.0	11b	6.7
10a	5.2	10e	6.1	10k	4.9	11b	3.5
10b	4.4	10e	2.7	10k	2.7	11b	4.3
10b	2.0	10f	8.3	10k	4.0	11b	4.1
10b	7.1	10f	10.6	10k	3.8	11b	5.2
10b	2.7	10f	6.0	10k	5.0	11b	3.5
10b	7.7	10f	3.8	10k	11.1		
10b	3.8	10f	10.6	10m	10.4		
10b	1.5	10f	4.3	10m	8.0		
10b	9.4	10g	5.6	10m	5.1		
10c	5.1	10g	6.8	10m	4.0		
10c	3.0	10g	3.6	10m	15.0		
10c	7.8	10g	3.5	10m	4.6		
10c	2.9	10g	4.4	10n	6.8		
10c	2.2	10g	4.7	10n	5.5		
10c	3.9	10g	4.0	10n	4.6		
10c	1.6	10h	3.9	10n	2.9		
10c	4.0	10h	6.2	10n	5.3		
10d	4.9	10h	2.5	10n	3.2		
10d	2.9	10h	3.4	10n	8.7		
10d	4.7	10h	2.7	10n	5.4		
10d	9.6	10h	2.5	10n	5.0		
10d	4.2	10h	2.9				
10d	6.5	10h	3.4				
10d	6.4	10i	2.5				
10d	7.3	10i	4.0				
10d	4.5	10i	3.3				

Table 25. Mica thickness measurement (μm), $LiNO_3$ leach 4 and 8 hours.

$LiNO_3$ Leach 4 hr Micro								$LiNO_3$ Leach 8 hr Micro					
12a	3.5	12d	7.8	12h	2.7	12p	5.2	5a	4.3	5f	4.6	5i	4.1
12a	5.5	12d	3.5	12i	3.0	12r	2.7	5a	3.8	5f	2.1	5i	2.5
12a	3.5	12d	5.5	12i	4.9	12r	2.5	5a	1.8	5f	2.0	5k	2.0
12a	3.6	12d	1.8	12i	5.2	12r	4.2	5a	3.5	5f	2.5	5k	3.6
12a	6.0	12e	4.0	12i	2.2	12r	4.2	5a	4.0	5f	2.9	5k	5.0
12a	1.5	12e	3.5	12i	3.6	12r	5.7	5a	2.5	5g	2.5	5k	4.6
12a	4.0	12e	3.5	12k	2.5	12r	4.7	5a	2.0	5g	5.0	5k	3.1
12a	15.8	12e	6.7	12k	3.5	12r	4.0	5a	2.2	5g	3.2	5k	1.1
12a	3.1	12e	2.7	12k	4.3	12r	3.0	5b	2.5	5g	1.1	5k	3.5
12a	6.7	12e	3.1	12k	4.1	12s	2.5	5b	3.8	5g	1.8	5k	4.0
12a	4.5	12e	3.2	12k	4.0	12s	3.5	5b	2.7	5g	6.0	5k	7.5
12a	3.1	12e	4.5	12k	3.6	12s	3.0	5c	3.6	5g	2.2	5k	4.2
12b	7.0	12e	4.0	12m	3.3	12s	2.0	5c	4.6	5g	3.9	5m	4.0
12b	4.5	12e	3.6	12m	5.2	12s	2.5	5d	3.6	5h	3.6	5m	2.2
12b	2.0	12e	2.5	12m	3.9	12s	2.7	5d	3.5	5h	3.3	5m	4.2
12b	4.0	12e	4.0	12m	2.0			5d	3.1	5h	2.2	5m	3.8
12b	4.0	12e	3.3	12m	2.8			5d	3.1	5h	3.8	5m	2.0
12b	2.5	12e	3.6	12m	2.7			5d	4.2	5h	4.4	5m	3.6
12b	5.0	12e	2.5	12m	4.0			5d	5.3	5h	3.8	5m	4.7
12b	4.9	12f	2.0	12o	3.5			5d	2.2	5h	2.5	5m	3.6
12c	7.1	12f	4.2	12o	4.2			5d	4.0	5h	2.5	5m	3.3
12c	5.5	12f	5.6	12o	5.1			5d	4.4	5h	6.5	5m	4.2
12c	8.8	12f	7.2	12o	4.2			5d	5.0	5h	5.3	5m	4.1
12c	4.4	12f	12.5	12o	5.1			5e	2.8	5h	2.0	5m	3.9
12c	5.1	12f	4.2	12o	3.0			5e	3.3	5i	3.0	5m	1.6
12c	5.1	12f	5.0	12o	4.2			5e	2.5	5i	2.5	5m	4.1
12c	6.2	12f	4.1	12o	3.6			5e	2.0	5i	4.0	5m	3.2
12c	4.7	12f	2.7	12p	3.3			5e	1.8	5i	3.8	5m	3.0
12c	3.8	12f	5.3	12p	4.1			5e	5.7	5i	2.1	5m	3.9
12d	2.2	12f	2.5	12p	3.6			5f	2.8	5i	6.0		
12d	2.2	12f	1.8	12p	6.0			5f	3.2	5i	5.2		
12d	2.9	12g	5.1	12p	5.0			5f	4.6	5i	3.5		
12d	3.0	12h	3.1	12p	2.5			5f	2.0	5i	6.0		
12d	2.0	12h	3.3	12p	3.9			5f	3.6	5i	6.8		

Table 26. Mica thickness measurement (μm), $LiNO_3$ leach 8 hours with no microwave.

$LiNO_3$ Leach 8 hr No Micro					
6a	4.4	6e	6.3	6k	4.0
6a	6.0	6e	3.2	6k	3.2
6a	8.5	6e	2.5	6k	3.6
6a	8.8	6f	2.1	6k	5.3
6a	4.6	6f	2.5	6k	4.6
6a	4.9	6f	2.9	6k	2.0
6a	4.0	6f	4.3	6k	6.5
6a	7.3	6f	3.1	6m	4.7
6a	3.0	6f	2.9	6m	6.0
6a	6.0	6f	2.8	6m	3.5
6a	5.1	6f	2.7	6m	5.4
6a	6.9	6f	3.2	6m	2.5
6b	4.6	6f	3.5	6m	4.1
6b	3.2	6f	2.7	6m	6.5
6b	9.1	6f	4.0	6m	3.3
6b	5.8	6f	3.3		
6b	3.5	6g	7.1		
6c	11.1	6g	7.1		
6c	3.6	6g	2.2		
6c	8.8	6h	3.6		
6c	4.1	6h	3.5		
6c	3.6	6h	5.2		
6c	2.8	6h	5.0		
6c	4.9	6i	4.6		
6c	2.2	6i	3.6		
6c	4.6	6i	6.2		
6c	4.4	6k	2.2		
6c	3.9	6k	7.8		
6d	2.5	6k	4.1		
6d	7.5	6k	3.2		
6d	10.7	6k	2.5		
6d	3.0	6k	3.5		
6e	3.6	6k	5.2		
6e	3.8	6k	3.2		

Appendix B Computer CD SEM Images

SEM Images Feed Sample, HCl Leach, Lithium Nitrate Leach

The following SEM images on the attached CD are of muscovite mica plates. These images are of the mica feed sample, grind test baseline, HCl leach test, and lithium nitrate leach test.